Analyses of the magnitude and frequency of a 400-year flood record in the Fish River Basin, Namibia

Article *in* Geomorphology · August 2018

DOI: 10.1016/j.geomorph.2018.07.025

Analyses of the magnitude and frequency of a 400-year flood record in the Fish River Basin, Namibia

G. Cloete[1]*, G. Benito[2], T. Grodek[3], N. Porat[4] and Y. Enzel[5]

1-Principal Civil Engineer, Knight Piésold Consulting Engineers, Windhoek, Namibia

2- National Museum of Natural Sciences (MNCN), Spanish Research Council (CSIC), Madrid, Spain

3-Department of Geography, The Hebrew University of Jerusalem, Mt Scopus, Jerusalem, 91905, Israel

4- Geological Survey of Israel, Jerusalem, Israel

5-The Fredy and Nadine Herrmann Institute of Earth Sciences, The Hebrew University of Jerusalem, Israel

*Corresponding author. Tel.: +264 61 307297; Fax: +264 61 307 298; Email: gcloete@knightpiesold.com

DOI: 10.1016/j.geomorph.2018.07.025

Abstract:

Ephemeral rivers in dryland regions exhibit a high interannual variability of streamflow regime, mainly dominated by floods. In these environments, floods are a water resource and a potential hazard with important socioeconomic implications. The Fish River (86,600 km^2) is the largest ephemeral stream in Namibia and, recently, also the focus of new development plans, including construction of the largest dam in Namibia. The hydrological analysis to support decisions implies large uncertainties owing to spatial-limited and short hydrological records (since 1962). Here we investigate the current and past patterns of extreme floods combining instrumental, historical, and palaeoflood records. Palaeoflood studies were performed at two reaches with preserved sedimentary evidence: at the upper sector (Vogelkranz) upstream of Hardap Dam (~13% catchment area) and in the lower part of the river, in the Fish River Canyon National Park (70% catchment area). In the Hardap reach, the palaeoflood record identified at least eight large floods during the last 350 years, with the largest flood reaching a minimum discharge of 4800 m^3s^{-1} (150-year return period). In the Fish River Canyon reach, the sedimentary record shows at least 12 large floods over the last 400 years, the largest with an estimated minimum discharge of 8700 m^3s^{-1}. The elevation of alluvial surfaces without flood evidence provided an upper bound for flood stages, associated with discharges of 6400 m^3s^{-1} and 16,140 m^3s^{-1} for the upper and mid-lower Fish River respectively. In the upper reach, the flood frequency analysis (FFA) combining systematic and palaeoflood data provided lower discharges (~25%) of the flood quantiles than the ones using only systematic data sets. In the Fish River Canyon reach, incorporation of the palaeoflood data into the FFA results in slightly higher values in the magnitude of the higher flood quantiles (~4-7%). The FFA analysis using an upper limited lognormal distribution function (LN4) fitted with palaeoflood data shows a good performance with a slow behaviour approaching the upper limit. Our flood frequency results suggest that the Hardap Dam should increase the spillway capacity and safety check flood of the original design in order to satisfy the dam safety criteria. However, the projected reevaluation figures calculated from conventional hydrological methods results in an overestimation of the safety floods according to our estimations.

Keywords: palaeoflood; hydrology; ephemeral rivers; flood frequency analysis

1. Introduction

Namibia, the most arid country in sub-Sahara Africa, experiences frequent droughts and has spatially unevenly distributed water resources. Water is among the most limiting factors in the development and in increasing the standard of living in Namibia and nearby countries (Heyns, 2005). Irregular flow in rivers complicates the effectiveness of a national water resource monitoring system as the calibration of water level recorders is challenging without water (Jacobsen et al., 1995). Indeed, Namibia's ephemeral rivers provide 22% of the national water supply, maintaining important plant and animal ecosystems (MAWF, 2008). In this dryland environment, floods are the generators of large volumes of water for surface reservoir storage and for recharge into subsurface aquifers (Dahan et al., 2008; Morin et al., 2009). These floods and their causative rainstorms are equally a water resource and a natural hazard. Therefore, flood hydrology research is critical to maximize the benefits of water resources and minimize the risk (Benito et al., 2010, 2011a).

The case of Namibia can be extrapolated to nearby South Africa and Botswana and to other desert regions worldwide. As water resources are central to the livelihood of inhabitants, dam projects and associated water schemes have been recently proposed to improve socioeconomic development (MAWF, 2008). The runoff potential of the Fish River (Fig. 1) is larger than other rivers flowing east or west, through or into the Kalahari or Namib deserts respectively. Therefore the largest dams in Namibia were built on the Fish River. The Hardap Dam (Fig. 1) is the largest in Namibia with a storage capacity of 295×10^6 m^3, completed in 1962, to provide water to the town of Mariental and to an irrigation scheme downstream of the dam. Farther downstream, the planned storage of the Neckertal Dam is 857×10^6 m^3 (completion by November 2018). Generally dam design and potential storage capacity depend on the length and quality of hydrological data, which are relatively sparse in Namibia. Where these data exist, gauging records are limited to about 65 years at most. Therefore, the largest and rarest floods are potentially underrepresented, and thus the distribution of all magnitudes of floods through time is poorly constrained. This situation complicates decisions related to utilization of floodwater resources and flood hazards.

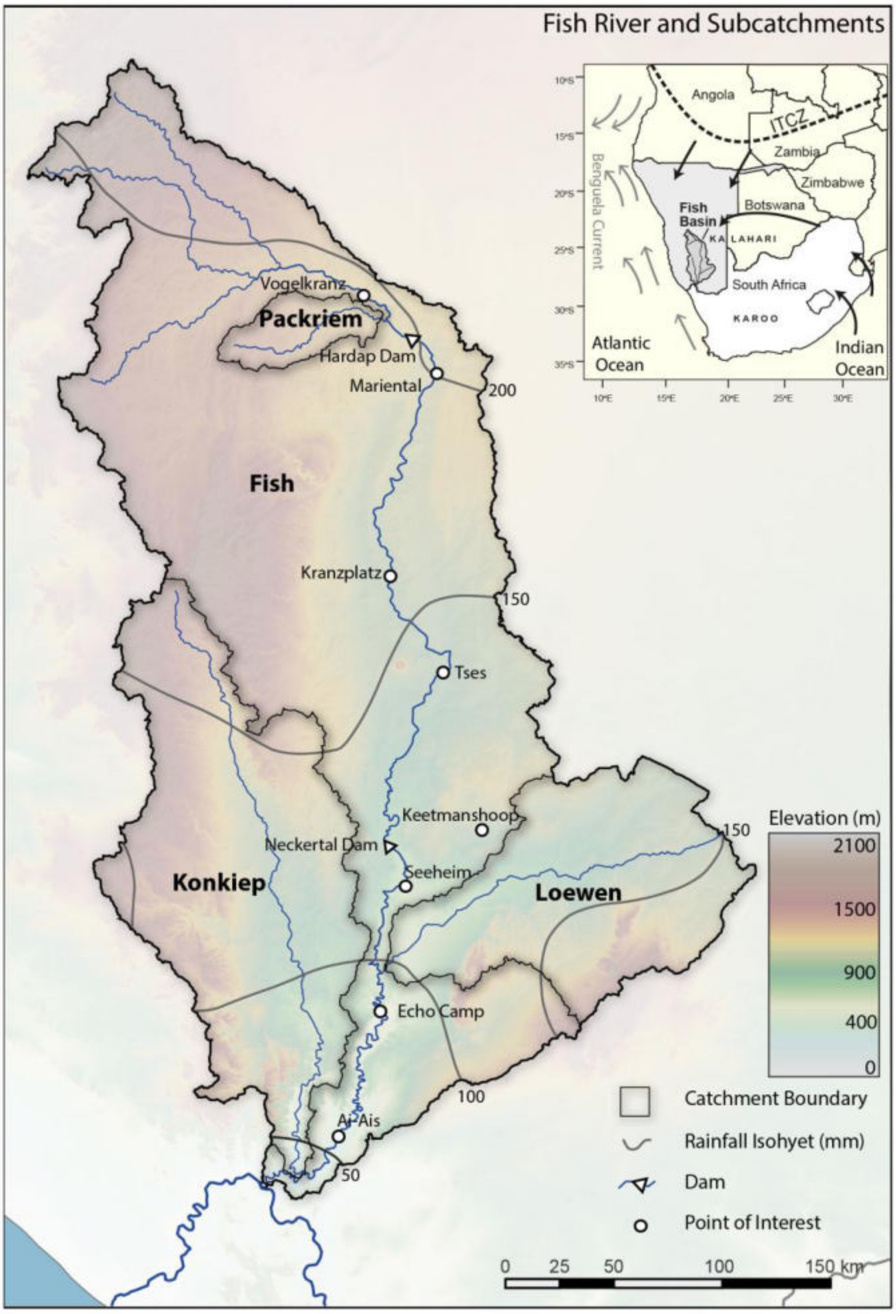

Fig 1. The Fish River catchment area within Namibia. The map shows the major drainage network, rainfall isohyets, hydrometric stations, dams, and weirs and the studied palaeoflood sites. Inset: Location of the study area within southern Africa and indication of the major ocean currents (dashed gray arrows) and the main atmospheric circulation that brings moisture to central Namibia during the austral summer (black arrows).

Hydrological data can be supplemented with records of extreme floods obtained by using palaeoflood hydrology and records of historical floods derived from written chronicles or direct observation. Palaeoflood hydrology relies on identification of evidence of flooding in conjunction with application of hydrodynamic principles to determine flow magnitude (Baker, 1987). Two basic types of physical palaeoflood evidence are high-water marks (HWM) and paleostage indicators (PSIs). High water marks includes mud, silt, seed lines, and flotsam (e.g., fine organic debris, grass, woody debris) that closely mark peak flood stage. This type of evidence typically only persists for weeks in humid climates and for decades in semiarid and arid climates (Williams and Costa, 1988). In contrast, palaeostage indicators provide longer lasting evidence of peak flow stages and typically consist of fine-textured flood sediment (slackwater flood deposits), gravel and boulder bars, silt lines, erosion features (Kochel and Baker, 1988; Webb and Jarrett, 2002), and botanical evidence such as scars and other damage (such as bent stems) on riparian trees. Depending on the environment, such evidence can persist for several millennia. Discharge estimates for these palaeofloods can be calculated under the assumption that the position of paleostage evidence (HWMs and PSI) relates closely to the maximum stage attained by an identified flood (Jarrett and England, 2002). Palaeoflood discharges can efficiently extend the flood data beyond the gauge/instrumental records and provide robust data for the design of dams and long-term quantification of floodwater resources (Benito and O'Connor, 2013).

The aims of this paper are to (i) extend the record of large floods by reconstructing palaeoflood stages and chronologies and estimating their magnitudes and frequency — this will also allow planners to base their decisions on longer-term flood records; (ii) provide information on the single largest flood/palaeoflood and to document the field-based, upper bound of this and other large floods in a specific time interval; (iii) construct a regional bound for flood magnitudes; (iv) evaluate the temporal pattern of large magnitude floods and their variability in relation with secular changes in climate; (v) estimate the regional maximum flood potential for the Fish River for dam design purposes. This will include traditional flood frequency analyses together with palaeoflood and upper bound information.

2. Study area

2.1. Geographical, climatic, and geological settings

The Fish River heads in the Naukluft Mountains in central Namibia and drains into the Orange River (Fig. 1). The catchment area is 86,600 km^2, and its main channel is 870 km long. The average slope of the Fish River mainstream from its origin until its confluence with the Orange River is ~2.2% (Crerar and Maré, 2005).

The climate varies from semiarid in the high plateau headwaters to the north (1000-2000 m above sea level, asl) to hyperarid at the low-lying central and southern portions with the driest conditions at the junction with the Orange River (70 m asl) (Fig.1). The fish River has two major tributaries, the Konkiep and the Lowen rivers, which make up ~35% of the total catchment area. Floods are mostly generated in the semiarid headwater where mean annual rainfall is 250 mm. In the southern parts of the watershed, mean annual rainfall is 50 mm (Mendelsohn et al., 2002). Rainfall is generated by convective storms during October to April (Austral summer). No large alluvial aquifers are located along the Fish River, groundwater storage is limited mainly to the channel downstream of Hardap Dam. The dominant vegetation on the Fish River catchment is classified as dwarf shrub savannah (Strohbach, 2001). The Fish River corridor contains riparian woodlands along river banks, and the sparse vegetation of the riverbeds and floodplains is subjected to regular flooding and water flow.

Geologically, the watershed is located in the western margin of the Kalahari Craton, comprising a stable granitic-gneissic coring a large portion of southern Africa (Geological Survey, 1980). This Craton is overlaid by sedimentary and volcanic rocks that cover the Precambrian-Cambrian boundary (Swart, 2008). The landscape in the upper-northern Fish River drainage basin is relatively flat. In the middle-lower reaches, the channels are incised deeply into the plains and into the underlying basement bedrock, forming the Fish River

Canyon. The Fish River Canyon is one of the largest river canyons in the world (the largest in Africa). It is 68 km long, 4 km wide, and 0.5 km in depth. In this canyon, the river level drops from 425 to 250 m asl.

2.2. Hydrometric data

Water levels in the Fish River have been recorded systematically by the Namibia Department of Water Affairs (DWA) at a weir at Seeheim since 1961 (coordinates 26°49'05" S, 17°47'30" E, altitude 700 m asl) and at flow gauging weirs Tses (coordinates 25°54'20" S, 17°58'36" E, altitude 910 m asl) and Ais-Ais (coordinates 27°54'41" S, 17°29'28" E, altitude 210 m asl) since 1976 (Figs. 2B-C). Measurements at all three of these stations continue to date; however, gaps in the data are common. These three gauging stations are located in the middle to lower Fish River. The Hardap Dam, located in the upper Fish River (coordinates 24°29'58" S, 17°51'31" E, altitude 1127 m asl), was constructed in 1962 and is used indirectly to measure inflow hydrographs and flood peaks (Fig. 2A). Prior to the construction of the dam, the Kranzplats hydrological station (Fig. 1) recorded flood events. The 18-year record from Kranzplats station was used in the original design of the Hardap Dam. No other flow gauging structures monitor the upper Fish River.

The largest recorded flood peak at Seeheim was 8300 m^3s^{-1}, measured in 1972 (Fig. 2C). In the same year, the largest recorded flood passing through the Hardap Dam was estimated by the Namibia Department of Water Affairs (DWA) at 6400 m^3s^{-1} (Fig. 2A) and at 6800 m^3s^{-1} by Hattingh et al. (2011). In our study, a new analysis of reservoir storage (derived from graphical dam level record), gate release and emergency spill release, give an estimate of peak inflow of 5500 m^3s^{-1}. The other two flow-gauging weirs, at Ais-Ais and Tses, were constructed four years later, in 1976, and recorded their respective largest floods in the years 2000 (4300 m^3s^{-1}) and in 1988 (2920 m^3s^{-1}) (Figs. 2B-D). The intense orographic rainfall leading to flooding is a result of warm, moist air from the east rising over the escarpment area, with a maximum 3 days accumulated rainfall of 191 mm at Hardap Dam (record interval 1983-2001) and 137 mm at Mariental (1918-2003). All the major rains and floods recorded during the instrumental period occurred during summer months (January to March).

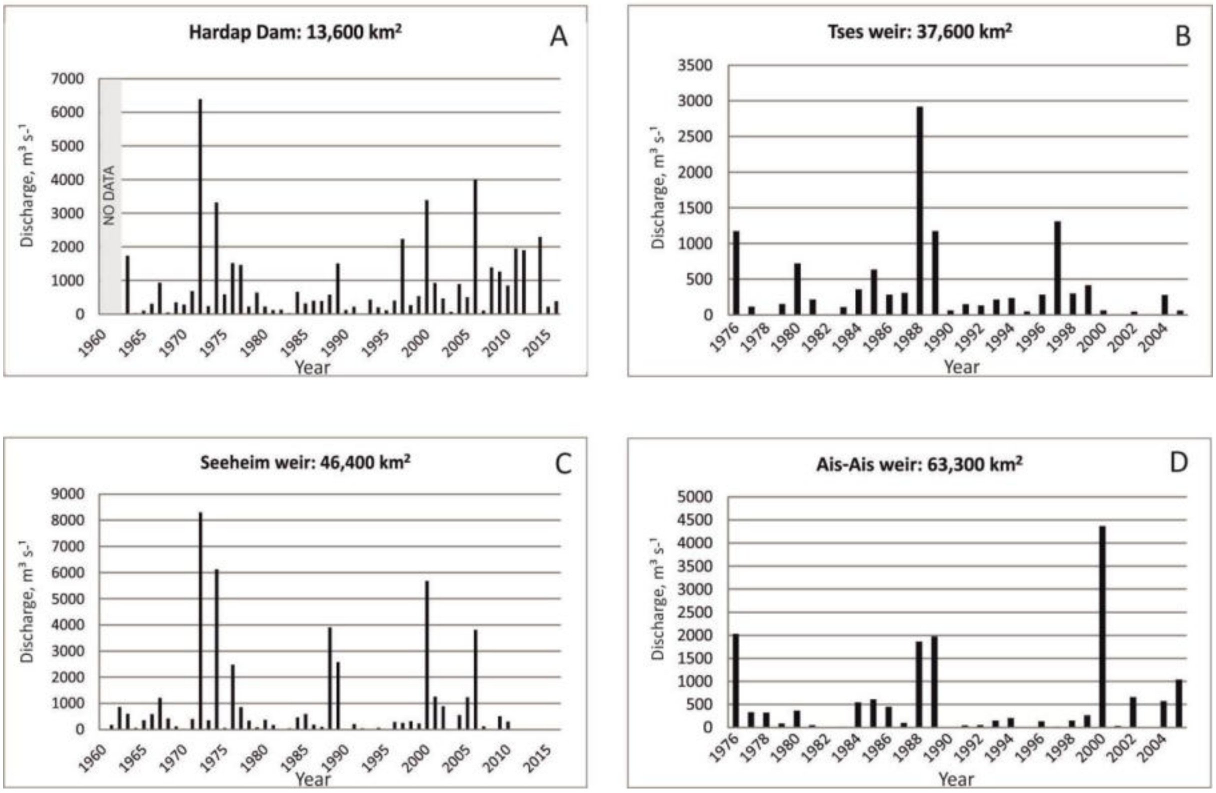

Fig. 2. Annual flood peaks from systematic flow data records along the Fish River. Locations of measurement stations are located in Fig. 1.

2.3. Historical floods

Historical records of earlier large floods on the Fish River are scarce and mainly available since 1908/1909 (Stengel, 1972; Table 1). In the Kuiseb and other Nambian rivers, historical flood records can be traced back to the early nineteenth century (Stengel, 1964); but these cannot be reliably extrapolated to the Fish River. Additional climatic information about years or periods of increased rainfall and droughts may be indicative on the timing of historical flooding. Nicholson (2001) compiled regional written documentary from missionary stations combined with historical gauge data for the nineteenth century providing a climate index class

(-3 for extremely dry to +3 for extremely wet) for 90 regional areas in Africa. The Fish River catchment is included within two regions: covering the upper catchment (region centre at -24º2’ S, 17º4’ E) and the middle-lower catchment (centre at-26º4’ S, 17º0’ E). Fig. 3 shows the rainfall index for the upper Fish catchment over the nineteenth century, and the annual rainfall recorded in the Keetmanshop station (1900-2016). In the instrumental record, large floods occurred in years with total rainfall amounts above the annual average (e.g., 1923, 1934, 1974; Fig. 3) although not all wet years recorded a large flood. The historical reports described regional rainy conditions in 1848-1849, 1862-1864, 1872-1874 and 1892-1894 (Nicholson, 2001; Fig. 3). These rainy periods together with 1814 and 1831 were reported as very wet years in the upper and middle Fish River catchment, perhaps a representation of periods of large floods (Fig. 3).

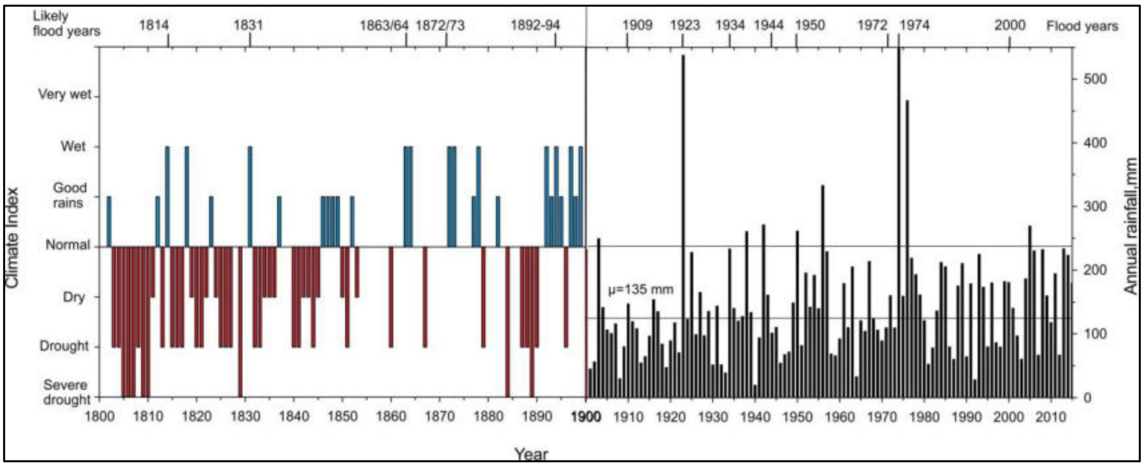

Fig. 3. Rainfall record of the Keetmanshop station (1900-2016, black line) and rainfall anomaly classes (red bars: severe drought/dry years; blue bars: wet/normal years) from regional rainfall class values obtained from documentary records after Nicholson (2001). Rainfall-anomaly class values: -3 severe drought year; -2 drought year; -1 dry year; 0 normal year; +1 good rains; +2 wet year. Years with insufficient evidence are not plotted. Most likely documented flood years during anomalous wet (+2) conditions are indicated in the upper *x*-axis. Since 1900, flood years were reported on gauge stations and weirs.

3. Methods

The methodological steps in our palaeoflood analysis include (Benito and O'Connor, 2013): (i) initial interpretation of aerial photographs and topographic maps of various scales to identify suitable sites for such analyses; (ii) field visit and survey for the identification and selection of specific research sites and to identify suitability of flood deposits and other evidence; (iii) stratigraphy of these deposits with emphasis on identifying flood units; (iv) sampling for chronology; (v) topographic survey of flood sites and river reaches; (vi) hydraulic modelling of the measured reaches and discharge estimation; (vii) comparison with available historical data; (viii) flood frequency analysis; and (ix) incorporation of the results into applied hydrology, engineering design, and water management.

Selected palaeoflood sites are located upstream of the Hardap Dam (Vogelkranz site) and within the Fish River Canyon (Echo Camp site). In both sites, the river flows in channels constrained by bedrock or consolidated alluvium to ensure stable channel geometry through time, which is critical to produce robust discharge estimations from hydraulic modelling. The fieldwork entailed identification of flood evidence of water levels (palaeostage) reached or exceeded during large floods, with an emphasis on sedimentary evidence (slackwater flood deposits; Baker and Kochel, 1988; Baker et al., 2002). Stratigraphic and sedimentological analyses of the deposits were carried out in the field and in the laboratory. Individual flood units were identified through a variety of sedimentological indicators (Baker and Kochel, 1988; Benito et al., 2003), namely the identification of clay layers at the top of a unit, erosion surfaces, bioturbation indicating the exposure of a sedimentary surface, angular clast layers where slope materials were deposited between floods, in addition to changes in sediment color. Apart from identifying individual flood units, sedimentary flow structures were also described to elucidate any changing dynamics during a particular flood and/or infer flow velocities that could improve discharge estimation (Benito et al., 2003).

Flood chronology was determined using radiocarbon and optically stimulated luminescence (OSL) dating (see Table 2). The accelerator mass spectrometry (AMS) radiocarbon dating was carried out by Beta Analytic. The OSL samples (Aitken, 1998) were analyzed at the Geological Survey of Israel. For OSL, sand samples were collected in the field using light-tight PVC cylinders, from which quartz particles with grain size of 88-125 µm were extracted from the bulk sediment samples using routine laboratory procedures (Porat, 2006). Approximately 5 mg of purified quartz was placed on 10-mm aluminum discs using silicon spray as an adhesive and 8- or 2-mm masks. Single aliquot measurements were done on either a refurbished Risø DA-12 or DA-20 TL/OSL reader, equipped with calibrated ^{90}Sr β sources. Quartz stimulation was carried out with blue LED, and detection was through 7-mm U-340 filters. The equivalent dose (*De*) was determined using the OSL signal and the standard single aliquot regenerative dose (SAR) protocol (Murray and Wintle, 2000), with between 18 and 30 aliquots measured for each sample. Preheats ranged from 220 to 260 °C; test dose was 4.5-5 Gy and a cut heat 20°C lower than the preheat was used to remove unstable signals. The OSL signal was measured at 125°C to background level. Dose rates were calculated from the concentrations of the radioactive elements K, U, and Th, measured on a subset of sediment sample by ICP MS (U&Th) or ICP-AES (K). Moisture contents were estimated at 5 ±2%, and the cosmic dose was estimated from current burial depths.

In addition to slackwater flood deposits (SWD), a field survey was completed with the identification of erosional landforms (stripped soils, flood scarps), high-flow channels, and evidence for nonexceedence stages of floods (e.g., preservation of undisturbed ancient colluvium). Recent large floods left abundant highwater evidence such as driftwood, which together with palaeoflood indicators were correlated to define the flood and palaeoflood water surface profiles along the river channel.

Applying the energy-based inverse hydraulic modeling on discrete palaeostage indicators (PSI), allows indirect determination of palaeoflood discharges (Baker, 2008). Discharge estimation by hydraulic modelling was carried out using the step-backwater method, the most commonly utilised method in palaeoflood hydrology (O'Conner et al., 1986; Webb and Jarrett, 2002). Computations were run using the HEC-RAS 4.1 one-dimensional flow model (Hydrologic Engineering Centre, 2010). Cross sections were surveyed along both study reaches using an RTK Global Positioning System (GPS) station set for post-processing data analysis where satellite visibility was poor. These surveys were tied with flood deposit elevations. At each cross section, signs of upper bound flood marks were also surveyed. The HEC-RAS model was used to convert the flood levels (palaeostage and upper bound indicators) into flood discharge to produce a hydrological data series.

The Vogelkranz and Echo flood discharges were calculated using Manning's *n*-values ranging from 0.025 for a relatively smooth channel in increasing steps of 0.005 up to 0.040. The Manning *n*-value that produced the best correlation between debris floodmarks, belonging to the same recent floods, and cross sections was 0.030 at Vogelkranz and 0.035 at Echo Camp. This range of n-values is in agreement with the *n*-values applied by Flood Studies Division of the South African Department of Water Affairs and Sanitation (DWS; Wessels, 2014). The DWS Flood Studies division concluded that a Manning *n*-value of 0.032 provides the most suitable results for extreme flood calculations in large southern African rivers. Past sensitivity analyses have shown that in reaches with hydraulic control, changes of up to +20% in Mannings *n*-value produce <5% change in corresponding flood discharge (Enzel et al., 1994). Rating curves relating individual flood unit elevations with HEC-RAS generated flood discharges were established for each site, and minimum flood discharges matching the upper elevation of sedimentary units were estimated in addition to the flood magnitudes associated with HWM and the nonexceedance bounds.

Flood frequency analysis was carried out at Vogelkranz and Echo Camp sites using the recorded data of the Hardap Dam and Seeheim gauge stations respectively combined with the palaeoflood discharge estimates. In order to combine the data for different sites on the same river (e.g., Vogelkranz site with Hardap Dam, and vice versa), the ratio of flood peaks were calculated as being the square root of the catchment:

$$Q_1 = Q_0 \sqrt{\frac{A_1}{A_0}}$$

where Q_0 is the discharge at Vogelkranz, Q_1 is the floodpeak entering the Hardap Dam, A_0 is the catchment area at Volgelkranz (11,050 km^2), and A_1 is the catchment area at Hardap Dam (13,600 km^2). The aim is to provide at the sites the statistical return period quantiles to estimate discharges associated with return periods of interest for flood hazard studies (from 50 to 500 years; e.g., Harden et al., 2011) and infrastructure design (>500 years). The first step in the methodological approach is the classification of the type of information gained by the palaeofloods (Stedinger and Baker, 1987; Botero and Frances, 2010). In the lower bound (LB) type it is known that the flood was larger than a known level (e.g., alluvial surface). For instance, in a flood deposit sequence this LB is the elevation (or associated discharge) of the respective SWD units overlying an alluvial or bedrock surface. This value remains as a minimal threshold during a period of time until a new bigger flood deposits a succeeding flood layer and therefore sets a new higher threshold. The upper bound (UB) data type represents information constraining the maximum possible discharge for a given flood or period of flooding. Such UB data typically are physically represented by the elevation of stable high alluvial or bedrock surfaces with lack of flood evidence (e.g., well-developed desert varnish on clast or bedrock surface indicative of high stability). The double censored (DC) data are defined by a bracketing discharge with its lower and upper limits corresponding to the value of the minimum discharge reached by the flood and the value of a maximum discharge not reached. The classification allows the incorporation of palaeoflood data into the available statistical procedure. To estimate the parameters of the probability distribution function, the maximum likelihood method was implemented (Stedinger and Cohn, 1986). A set of probability distribution functions were fitted to the systematic and palaeoflood data. The two-component extreme value (TCEV) distribution function produced the best fit.

4. Palaeoflood hydrology in the Fish River

At Vogelkranz (24°18'32" S, 17°38'19" E) (Fig. 1), on the farm 'The Analyst', the catchment area is 11,200 km^2, ~13% of the total catchment area of the Fish River drainage basin. The Echo Camp site (27°20'28" S, 17°42'09" E) (Fig. 1) is in the Gondwana Nature Reserve of the Fish River Canyon. Here the catchment area is 57,000 km^2, approximately 70% of the basin area.

4.1. Stratigraphy and chronology of the Vogelkranz site

In the Vogelkranz site, the stream bed (50-60 m wide) is incised on bedrock and consolidated alluvium and is composed by coarse gravel lag deposits and lateral gravel bars (Fig. 4). The left margin of the channel is bounded by a bedrock cliff with bouldery talus deposit accumulations at the toe, whereas the right bank cuts a gravel and boulder terrace with apparent stability to fluvial erosion (Fig. 5A). Three sequences of SWD were described along the 500−m reach. Sites VK-1 and VK-2 are located on a right bank gravel terrace, and VK-4 is placed at the mouth of a side tributary (Fig. 4).

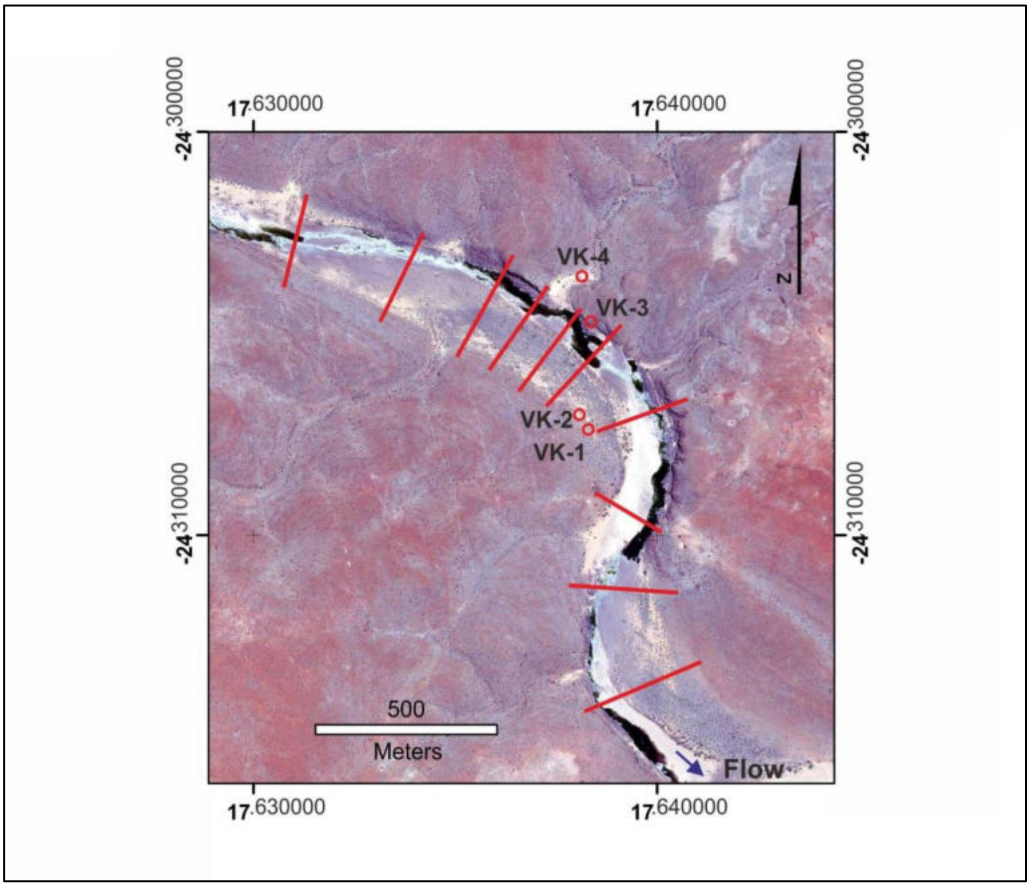

Fig. 4. The Vogelkranz site study reach in the Fish River (photo from Google Earth dated on 19 July 2016). The palaeoflood sediment stratigraphic profile sites and cross sections used in the hydraulic model discharge estimations are indicated.

The highest flood deposits at VK-1 are associated with estimated minimum discharges of 3460-3610 m^3s^{-1}. These SWDs are ca. 25 cm in thickness and are comprised of at least four units of fine to very fine sand with obscure lamination (Fig. 5B). The contacts between units 1-2 and 3-4 are formed by continuous silt laminae of ~3 mm in thickness, whereas contact at units 2-3 is diffused. The second and third flood units are 165 ±70 (A.D. 1845 ±70) and 55 ±35 years old (A.D. 1955 ±35) respectively (Fig. 6, Table 2).

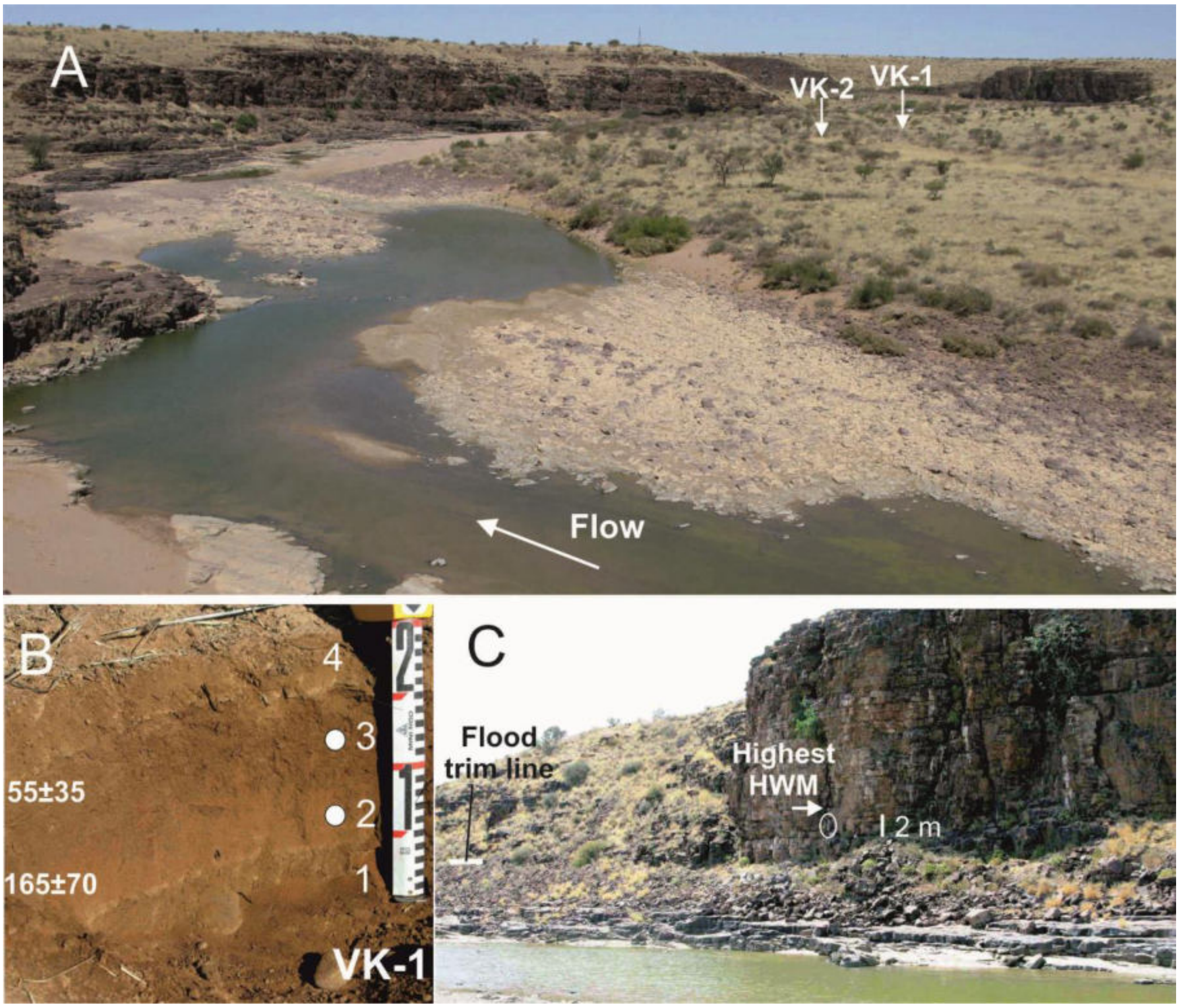

Fig. 5. Vogelkranz reach: (A) general view of the Vogelkranz reach looking downstream with location of stratigraphic profiles VK-1 and VK-2 on old alluvial surfaces. (B) View of the VK1 pit with indication of the stratigraphic units and luminescence dating results. (C) Flood trimline on coarse colluvium deposits, and location of the log stuck in a crevice against the cliff, dated by radiocarbon as 30 ±30 ^{14}C YBP

About 60 m upstream, profile VK-2 is lower in elevation with an associated minimum discharge of 2260-2500 m^3s^{-1}. The SWDs contains at least six flood units with a total thickness of 40 cm (Fig. 6). The lowest three units are silt to very fine sand with horizontal lamination and clear to diffuse contacts marked by bioturbation and an individual colluvial clast on the boundary. The upper set are comprised of very fine sand to silt texture and well-developed parallel to cross-lamination, with clear contacts caused by erosion or deposition of clay to silt laminae. The second and fifth flood units are 310 ±65 (A.D. 1700 ±65) and 235 ±35 (A.D. 1775 ±35) years old respectively (Fig. 6, Table 2).

The thickest palaeoflood deposits are located at about 130 m upstream from a tributary junction (VK-4). Minimum discharges estimated for this stratigraphic profile range between 1400 and 1560 m^3s^{-1}. This flood deposit bench contains at least seven flood units, with a total thickness of 1 m, made of silt to very fine sand, with blurred horizontal lamination, and a high degree of bioturbation and root marks, some filled with secondary carbonates (Fig. 6). The OSL samples were not dated because of the lower topographic position in relation to site VK-2 showing a similar number of flood units likely within an equivalent temporal framework.

In addition to SWD, high-water marks related to maximum flood stages are well preserved as scour lines on ancient colluvium at the left valley margin. This line elevation is also matched by a thin veneer of patchy sand deposits and remnants of drift wood (Fig. 5C). An organic sample (VK3; Beta-287852) was taken from a tree log stuck in a crevice against the left margin cliff. It was very young (30 ±30 radiocarbon YBP), corresponding to 2σ cal. age of A.D. 1890 to 1910 and cal. A.D. 1950 to beyond 1960. The fresh appearance and continuity of the scour marks and driftwood of this line suggest a likely correspondence to the 1972 flood, the largest on the instrumental record. Peak flow discharge estimation associated with this highest line is 4800 m^3s^{-1}.

An intensive field search was dedicated to identifying flood indicators higher than this presumed 1972 flood stage. The search also focused on the flat gravel surfaces within the limit of the highest evidence of flood stage along the study reach. We found no evidence for larger floods. These high alluvial surfaces are characterised by poorly developed soils or a thin veneer of patchy aeolian sands on the gravelly surface. We used these observations to provide a UB for flood stages in the reach of 6400 m^3s^{-1}. The duration of this nonexceedence UB is difficult to establish, but according to the weak soil development we estimate this time interval as possibly 1000 years.

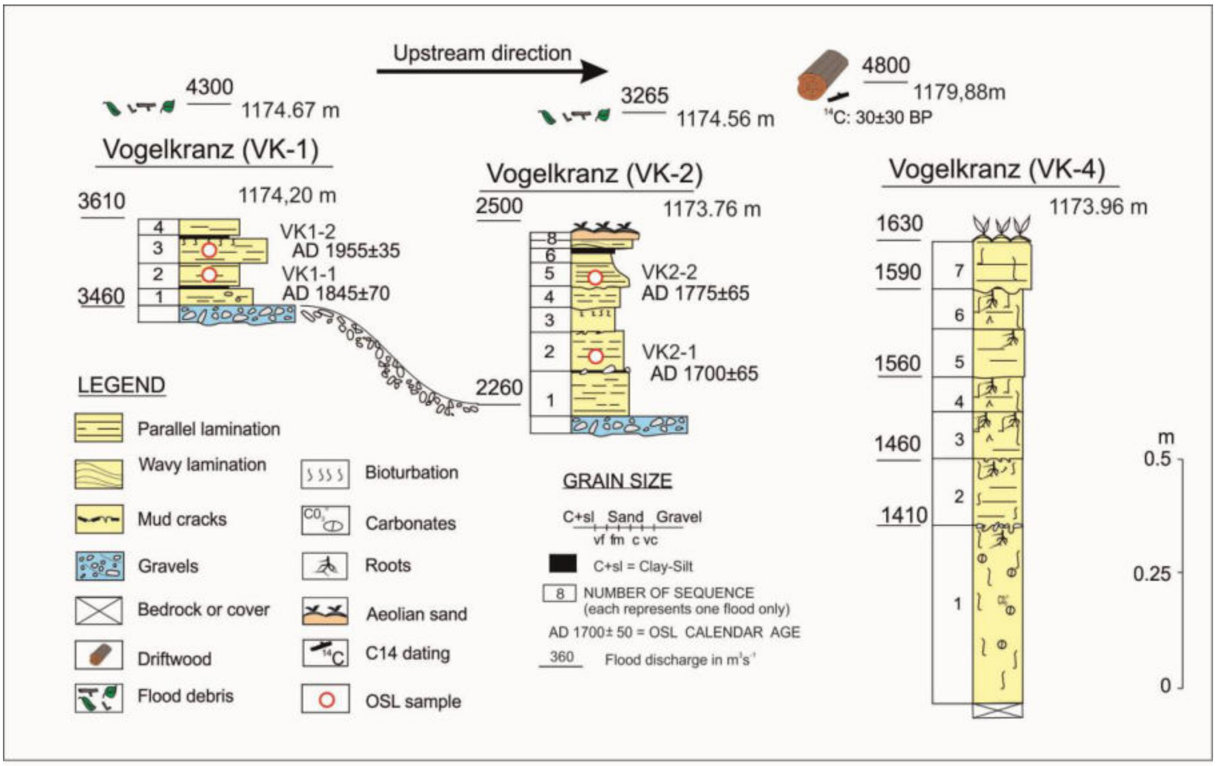

Fig. 6. Stratigraphic profiles described and sampled at the Vogelkranz reach, showing dated samples (OSL dates in years A.D., and radiocarbon dates in conventional $_{14}$C YBP). The GPS elevation (in m asl) of the stratigraphic profiles and flooddrift wood is indicated.

4.2. Stratigraphy and chronology Echo Camp

At the Echo Camp study site the catchment area is 57,000 km^2. The studied reach extends along a length of 1900 m with an average valley bottom width of 150-350 m (Fig. 7). The river valley develops a vertical cliff on the left margin with a significant tributary entering on the upper sector of the studied reach. The right valley margin descends in steps to the valley bottom, formed in several old river terrace surfaces with desert varnish coating the gravelly and boulder deposits (Fig. 8A). Six SWD sites were documented, with four providing relevant palaeoflood data: EC-1 and EC-2 are located on top of gravel alluvial surfaces, whereas SWD sites EC-4 and EC-5 are within the tributary valley (Fig. 7).

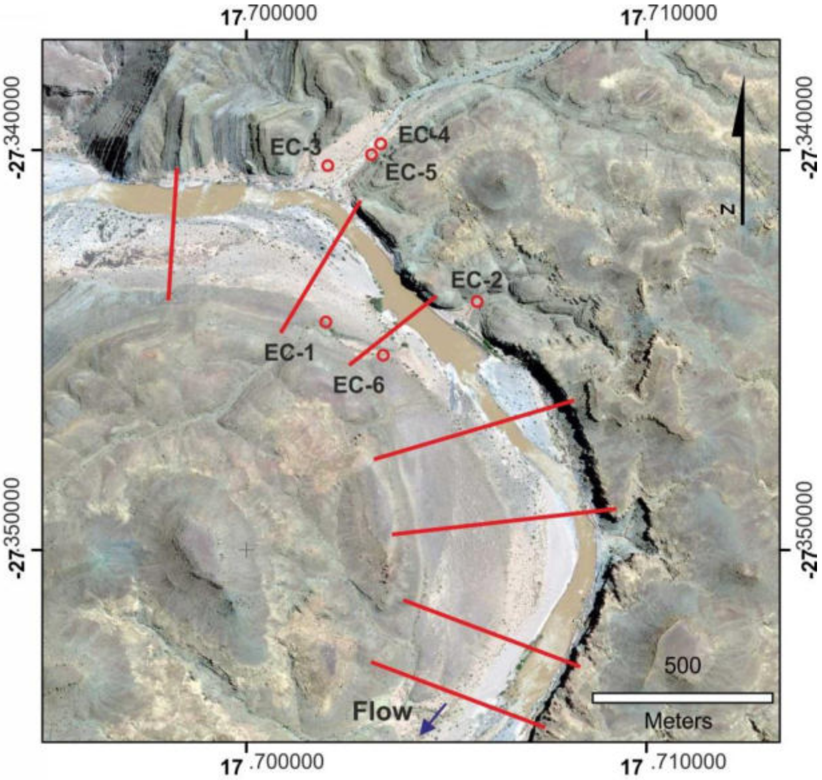

Fig. 7. The Echo Camp site study reach in the Fish River (photo from Google Earth dated on 23 December 2014). The palaeoflood sediment stratigraphic profile sites and cross sections used in the hydraulic model discharge estimations are indicated.

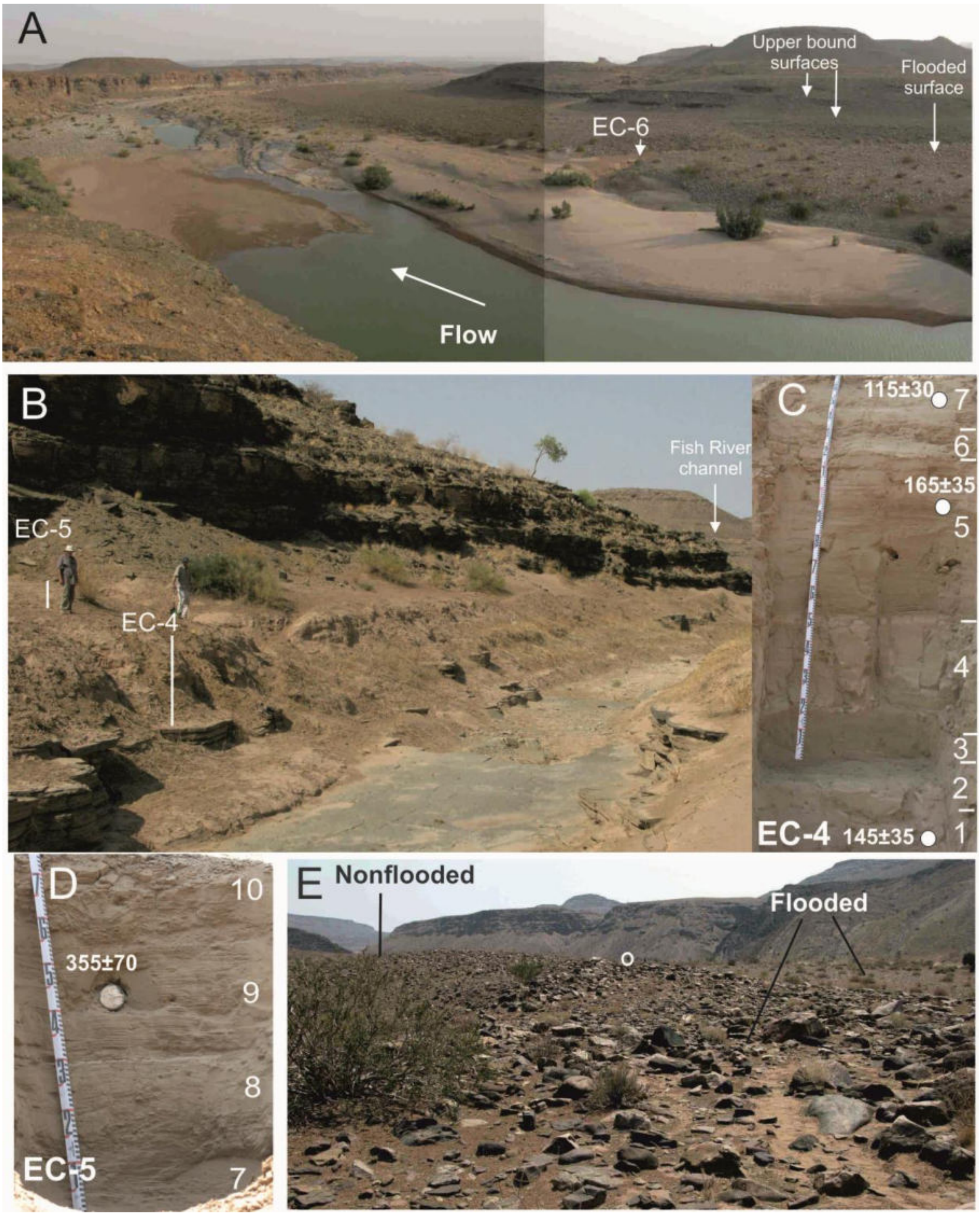

Fig. 8. Echo Camp reach: (A) general view of the Echo Camp reach looking downstream with location of stratigraphic profile EC-6 and old alluvial surfaces. (B) View of the flood bench along the tributary stream with indication of the location of stratigraphic profiles EC-4 and EC-5. (C) View of stratigraphic profile EC-4 and luminescence dating results. (D) Site EC-5.

(E) View of old alluvial surfaces with evidence of flood sands (foreground), and at the background those covered with desert varnish and likely above recent flooding.

Site EC-1 is located at the upstream section (350 m width) on an alluvial surface 13 m above the riverbed. On this surface, evidence of episodic flooding is recognised by unvarnished boulder deposits separated by a flood scar from a slightly higher alluvial surface with boulders coated by dark-brown desert varnish (Fig. 7). On the flooded alluvial surface, a trench was dug on a patch of fine sediments surrounded by gravels and boulders. Here, the stratigraphy shows two 6-cm-thick flood units, each composed of very fine sand and silt with ripple lamination (Fig. 9). These flood layers are capped by 2-mm-thick silt laminae with mud cracks indicating post-flood surface exposure. The upper flood layer is covered by unbedded aeolian sands. An OSL sample collected from the bottom flood unit yielded an age of 370 ±80 years (A.D. 1640 ±80). This sequence contains depositional evidence for the largest floods in this reach over the last 400 years, with a minimum discharge of 8690 m^3s^{-1}.

Sites EC-4 and EC-5 are located in a back-flooded tributary stream (90 m wide) entering the canyon (Fig. 8B). In this tributary, a 4-m-thick flood deposit bench can be traced 150 m upstream, thinning out as the channel rises in elevation upstream (Fig. 8B). A gully cutting the flood bench across the valley shows a two-dimensional exposure of the SWD stratigraphy. The EC-4 profile is composed of at least eight flood units characterised by fine and very fine sands with parallel to wavy lamination and ripple marks indicating up-tributary flow direction (Fig. 8C). The sand units are capped by 1-2 cm thick silt laminae. Some very fine sand to silt massive sediments (2-5 cm in thickness) between flood beds is interpreted as aeolian deposits. Profile EC-5 is on a transversal face of this bench showing a stratigraphic continuation of the EC-4 stratigraphy (Fig. 8B). The outcrop shows six flood units; only three (9 to 11) of them are not represented in EC-4 (Fig. 9). The sediments are composed of very fine sand to silt with parallel lamination (Fig. 8D). Three OSL ages from EC-4 are 145 ±35 (A.D. 1865 ±35; unit 1), 165 ±35 (A.D. 1845 ±35; unit 5), and 115 ±30 (A.D. 1895 ±30; unit 7). Unit 5 (A.D. 1845 ±35) is stratigraphically younger than unit 1 (A.D. 1865 ±35) which constrains unit 5 to an age between A.D. 1830 and 1880. The chronological framework of these deposits revealed younger ages than expected. Older flood deposits, if present, are likely buried by these younger deposits, but limited field exposures did not allow confirmation. The minimum flood discharges associated to bench elevation in EC-4 is 1450 m^3s^{-1}, whereas at EC-5 this discharge exceeded 1800 m^3s^{-1}.

Sites EC-6 and EC-7 are in a small tributary valley, deeply incised into the old alluvial terrace (Fig. 8A). The EC-6 stratigraphy shows at least 10 flood units, although the gravel bottom was not reached in the trench (Fig. 9). The flood units are fine to very fine sand and silt with parallel and wavy lamination. Sediments described at EC-7 abut the vertical face of the bench forming site EC-6. Site EC-7 shows at least three flood units with flood stages lower than the uppermost units in EC-6. Ages from EC-6 and EC-7 are not available — although its position, number of units, and stratigraphy resemble those described in EC-4 and EC-5 — and were likely deposited over the last 150 years. The estimated minimum discharges of these sites range between 1180 and 3400 m^3s^{-1}.

The presence of old alluvial surfaces at different elevations along the Fish River Canyon is a unique setting in searching for evidence of inundation and noninundation at elevations within the uppermost flood stage limit (palaeohydrological bounds; Levish, 2002; Figs. 8A, 8E). On several of these alluvial terraces along the study reach, soils and sediments were documented in dug pits with the goal of finding evidence of surface stability and/or flooding. The elevation of alluvial surfaces, without any flood evidence, provided a UB for flood stages, corresponding to an associated peak discharge of 14,900-16,140 m^3s^{-1}. These discharges are almost twice the largest flood discharge estimates from palaeoflood sediments at site EC-1 (8690 m^3s^{-1}).

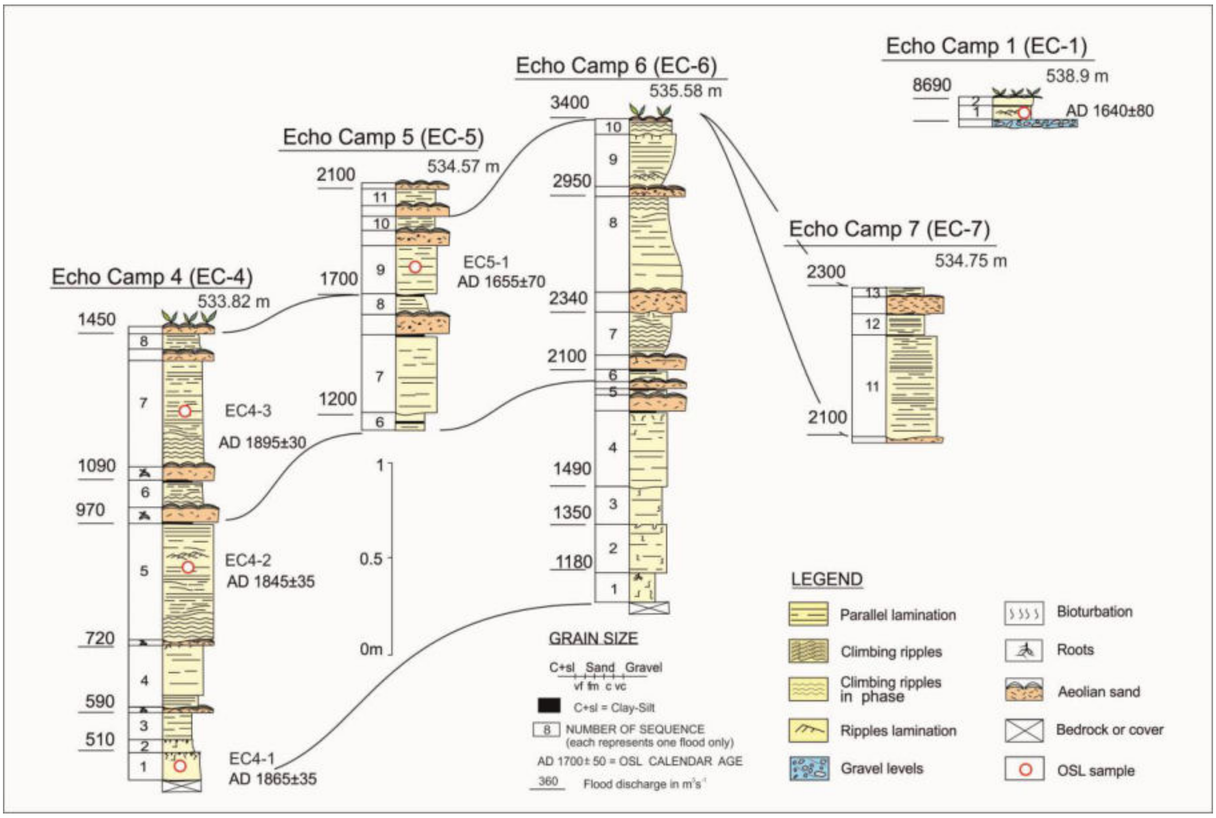

Fig. 9. Stratigraphic profiles described and sampled at the Echo Camp reach indicating dated samples (OSL dates in years A.D.) and proposed correlations between sections. The GPS elevation (in m asl) of the stratigraphic site is indicated on the upper right side of the profile.

5. Flood frequency analyses using palaeoflood data

Extreme value probability distributions were fitted to the annual series of maximum discharges (SYS) from instrumental records and to the combined sets of these annual series and the palaeoflood data (SYS+PALEO) to estimate values for several recurrence intervals. Several distributions were examined: exponential, lognormal, Gumbel, generalized extreme value (GEV), and two-component extreme value (TCEV). These distribution functions, however, provide quantile extrapolation without limit on discharge values, possibly exceeding the hydrometerological potential of the catchment to produce floods of such high magnitude (Enzel et al., 1993). Field expression of upper limits of flooding over a specific time interval, described above as palaeohydrological bounds, were used to constrain the tail of flood-frequency distributions (Levish, 2002; England et al., 2006). This UB gives more robust frequency and magnitude estimates of rare and large floods (O'Connell et al., 2002). Some distribution functions may incorporate an additonal parameter as an upper limit to the random variable (Botero and Frances, 2010). Here, we apply a UB distribution function to our case studies, namely LN4, that is a transformation of lognormal distribution (Takara and Loebis, 1996).

For the Vogelkranz reach in the upper catchment, eight palaeoflood discharges were included as LB types exceeding incrementally increasing discharge thresholds between 2260 and 3650 m^3s^{-1} over the time interval 1675-1962 (Fig. 10A). The systematic data from the Hardap Dam recorded three floods exceeding the highest palaeoflood discharge threshold, namely the 1972 (5500 m^3s^{-1}), 1973 (3320 m^3s^{-1}), and 2000 (3400 m^3s^{-1}) floods. Field evidence of the 1972 flood in the study reach is a tree log stuck in a rock crevise that provided a discharge of 4800 m^3s^{-1}. A more recent HWM (driftwood) corresponded to only one flood exceeding the coarse gravel terrace, meaning a discharge over 3300 m^3s^{-1}. These HWMs are likely associated with the 1972 flood, although it was possibly left by the second largest flood in the year 2000.

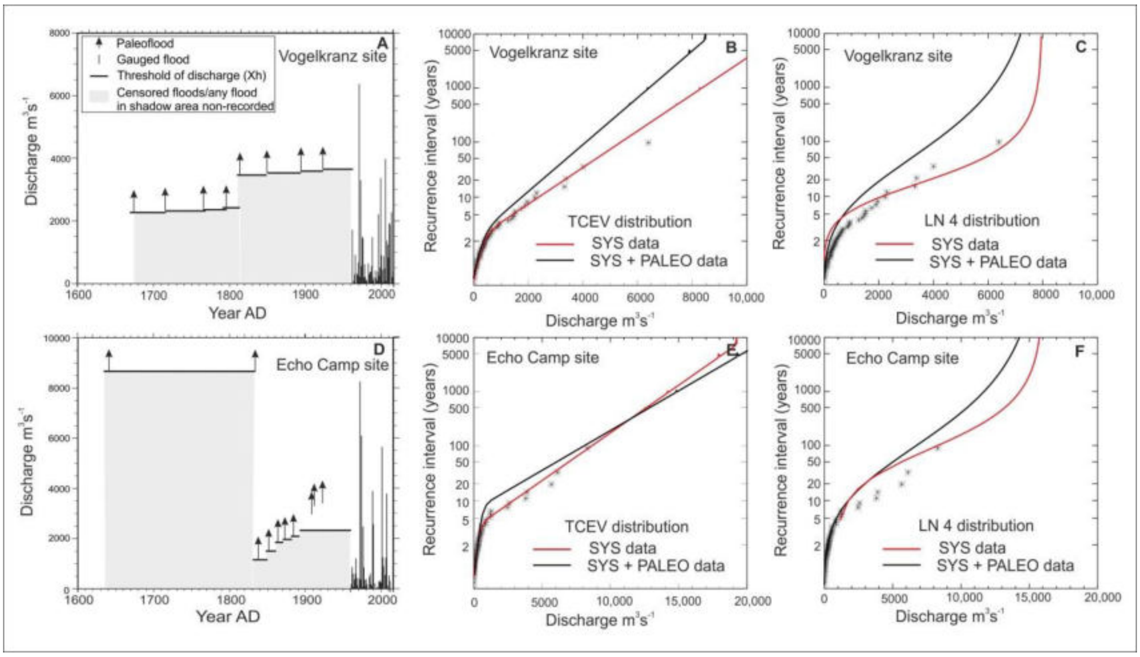

Fig. 10. Left column: palaeoflood and systematic discharges at Vogelkranz (A) and Echo Camp (D) sites. The horizontal shaded areas represent the discharge threshold values (Q_h) and the arrows the minimum discharge associated to the palaeoflood events used in the flood frequency analysis. Central column: two-component extreme value distributions fitted to annual series of systematic peak discharges and palaeoflood information for Vogelkranz (B) and Echo Camp (E). Right column: lognormal UB distribution function (LN4) fitted to annual series of systematic peak discharges and palaeoflood information for Vogelkranz (C) and Echo Camp (F).

The plotting positions of the Fish River show a change in the slope of the sample, the *dog-leg* effect (Potter, 1958), characteristic of torrential regime rivers (Fig. 10B). The TCEV distribution (Rossi et al., 1984) was found to best fit the data, since it provides a good representation of two flood populations; ordinary (e.g. local storms) and extraordinary floods (e.g. mesoscale convective systems). The incorporation of the palaeoflood data into the flood frequency analysis provided lower estimates for the flood quantiles. For instance, the 1%

annual exceedance probability (AEP) at Hardap Dam resulting from gauge data (5200 m^3s^{-1}) is about 15% higher than the one also using palaeoflood data (4415 m^3s^{-1}). These results are not unique, as in several cases longer records from historical or palaeoflood data may not always contain evidence for floods larger than experienced in the instrumental record (55 years) — although this is not the more common case. We also note that the annual floods from Hardap Dam were not obtained from a gauge station but from the rate of water input to the reservoir. Moreover, stream flow from the Pakriem River that joins the Fish River downstream of the palaeoflood study reach may contribute with a portion of the discharge entering the dam explaining, in part, the anomalously high peak flows recorded in the Hardap Dam. In the Vogelkranz reach, the field inspection of high alluvial surfaces provided a UB for maximum peak flow of 6400 m^3s^{-1}, which corresponds to the ~500-year flood in the instrumental record and the 2000-year flood using the palaeoflood record (Table 3). Note that the largest flood evidence in the study reach for an ~400-year interval (A.D.~1617 to 2015) was estimated at 4800 m^3s^{-1} which corresponds to average recurrence intervals of 100 years and 300 years from the SYS and the SYS+PALEO analyses respectively. In the FFA analysis using the UB distribution function LN4, the UB estimated by the field evidence as 6400 m^3s^{-1} matched the UB value calculated using the Kijko (2004) Generic Equation, in a similar fashion as described by Botero and Frances (2010). This UB value allowed the use of the SYS data and the comparison with the SYS+PALEO data at the Vogelkranz site and at Hardap Dam, considering the proportional increase on drainage surface. The LN4 function shows a good performance in the distribution fitted with palaeoflood data asymptotically approaching the upper limit (Fig. 10C). The discharge for quantiles equal or lower than the 100-year flood in the LN4 distribution for the SYS+PALAEO data set is similar to those obtained with the TCEV distribution (Table 3). The largest palaeoflood HWM (4800 m^3s^{-1}) is associated with an average recurrence interval of 300 years. The LN4 distribution function fitted only to SYS data also matches the flood data, but more rapidly approaching the upper limit than the one fitted to the SYS+PALEO record (Fig. 10C). The LN4 shows the best fit to the plotting positions, matching the dog-leg effect and the field evidence of the UB. This distribution is highly recommended for estimating the discharges associated to quantiles of interest for dam engineering in the Fish River catchment.

In the Echo Camp reach, the systematic records applicable to the Echo Camp reach are the Seeheim station (46,400 km^2, since 1961) and the Ais-Ais weir (63,300 km^2, since 1976), the former with higher annual maximum discharges owing to downstream flood peak attenuation. In frequency analysis, the Seeheim station was used because it has the longest systematic record and includes the 1972 flood, which is the largest on record. A total of 11 palaeoflood data were included in the FFA as LB type, 10 post-dating A.D. 1837 and two post-dating A.D. 1640, found on the upper alluvial surface (Fig. 10D). The data input was supplemented with the historical observation of water level for the 1912 flood at Seeheim, which was associated with a discharge of 3200 m^3s^{-1} according to our hydraulic calculations. The TCEV distribution function provided the best fit to the plotting positions, both using the SYS and the SYS+PALAEO data sets (Fig. 10E). The incorporation of the palaeoflood data into the FFA results in slightly higher values (~4-7%) in the magnitude of the higher flood quantiles (Table 3). The largest palaeoflood discharge of 8690 m^3s^{-1} is associated with an average recurrence interval of ~100 years, whereas the 1972 flood (8301 m^3s^{-1} at the Seeheim station) is slightly below that return period. The inspection of high alluvial surfaces, in search of flooded/nonflooded evidence, produced evidence that relates to a UB discharge of 16,140 m^3s^{-1}. This discharge, according to the TCEV distribution, would be exceeded by a 2000-year flood (exceedance probability of 0.05%), suggesting an unrealistic high value caused by artificial extrapolation of this unbounded parametric distribution function. The analysis of the PALEO+SYS data with an LN4 UB frequency distribution fixing the UB to 16,140 m^3s^{-1} provides a better performance, reproducing the shape of the plotting positions with a slow approach of the function to the upper limit (Fig. 10F). The largest palaeoflood of 8690 m^3s^{-1} is then associated with an average return interval of 250 years, consistent with the two floods recorded on the upper alluvial surface since A.D. 1640.

6. Discussion

6.1. Flood history and climatic context

The Fish River contains abundant sedimentary evidence of ancient floods deposited mainly at tributary mouths and expansion reaches and locally overlying high alluvial surfaces. The dry environmental conditions of the region favour the preservation, identification, and persistence of these fine-textured flood sediments and the contacts between flood units.

The atmospheric conditions leading to flooding are related to farther south than normal incursions of the semipermanent Angola low-pressure cell and moisture advected from the Indian Ocean and from the African tropics (Henschel et al., 2005, Grodek et al., 2013; Fig. 1). The abnormal moisture transport toward central and southern Namibia produces higher than average seasonal rain that may even penetrate the Namib Desert and cause regional flooding. The general hydrological response of the catchment during the largest floods is corroborated by mineralogical fingerprints from clay mineral assemblages (illite/chlorite ratio) of flood sediments south of Ais-Ais, which shows influence from different catchments (Heine, 1987; Heine and Vökel, 2010). This widespread flood response should also be reflected by the flood stratigraphy with a similar temporal framework and number of flood units. The most complete palaeoflood stratigraphy is found on tributary mouths and upstream of tributary valleys being backflooded during high flood stages. In the Vogelkranz site, the stratigraphy contains at least eight flood units, whereas in the Echo Camp site the tributary stratigraphy is composed of at least eleven flood units. However, palaeoflood sedimentation on high alluvial surfaces provides the most valuable palaeoflood data, allowing discernment of the number of floods exceeding the elevation of some high alluvial surface over a certain time interval. In the Vogelkranz site, eight and four flood sedimentary units were identified on two alluvial surfaces that require a minimum discharge of 2250 and 3500 m^3s^{-1} for inundation respectively. In the Echo Camp, two flood units deposited on a high alluvial surface show the number of exceedances for discharges higher than 8690 m^3s^{-1} over the last 350 years, providing critical data necessary for flood-frequency analysis. These discharges are comparable to the largest peak flows recorded in the instrumental record for the 1972 flood, namely 6400 and 8300 m^3s^{-1} respectively at the Hardap Dam and Seeheim gauge station, although we modelled this flood in the studied reach at Vogelkranz as 4800 m^3s^{-1} according to identified high-water marks.

The two studied palaeoflood sites agree on the timing of this past flood evidence, with the oldest palaeoflood age of 310 ±65 years. The relatively short time record indicates either an episodic erosion of older flood deposits by subsequent larger flooding or may indicate a preceding interval of unknown length without major flooding. Sedimentary preservation problems were also described on other palaeoflood studies on Namibian rivers (Heine, 2004; Heine and Völkel, 2011). For instance, in the lower Fish River south of Ais-Ais, Heine (1987) described at least two different accumulation phases of flood deposits, the youngest sequence deposited by the 1962/1963 floods, but without evidence of flood sediments deposited during the last centuries. Preservation of these deposits depends on the fluvial activity of tributary streams and slope runoff, resulting in flood benches composed of multiple inset relationships caused by cycles of erosion and aggradation in the valley.

During the overlapping historical interval (since A.D. 1800) and instrumental records (since 1962), a most likely date was assigned to each palaeoflood deposit coherent with bracketing ages provided by the numerical geochronology. The assigned flood ages allow plotting (Figs. 10A, D) but does not affect the flood frequency analysis results. In the Vogelkranz reach, four floods exceeding 3500 m^3s^{-1}, that post-date an OSL age of 165 ±10 years, were assigned to known rainy years at 1831, 1892-1893, 1923, and 1972. In the Echo Camp, the palaeofloods recorded at the tributary stream post-date an OSL age of 145 ±35 years and the overlying seven to eight flood deposits probably occurred during the nineteenth century. Likely they occurred in anomalous rainy years of 1814, 1831, 1863, 1863-1864, 1872-1873, 1892-1893, 1894, and 1898, according to regional historical data of wet years in the Fish River catchment (Nicholson, 2001). Another set of flood units were deposited since 1900, with likely dates of 1909, 1923, 1972, 1976, 1988, 2000, and 2006, all with discharges over 2500 m^3s^{-1}.

The palaeoflood chronology shows a period of flood activity in the Fish River at A.D. 1640-1700 that climatically corresponds to the Little Ice Age (LIA; A.D. 1300-1800; Tyson et al., 2000). Similarly, increased moisture conditions during 1550-1700 and 1825-1900 were recorded from middens of rock hyrax (*Procavia capensis;* Chase et al., 2009) in the Namib Desert. In the central Namib (Swakop, Kuiseb, and Tsauchab rivers), evidence is seen of flooding during the LIA, but field data suggest palaeoflood magnitudes minimally exceeded, if at all, the most recent floods (Heine, 2004, 2011). In the Swakop River (Greenbaum et al., 2014), the largest flood magnitudes were recorded between A.D. 1300 and 1850 and relate to the transition from a drier climate to a colder and probably wetter climate during the LIA in southern Africa (Tyson and Lindesay, 1992; Heine2004). In the Kuiseb River only minor changes in flood frequency were identified over the past millennium, with an increase in the occurrence of large floods at A.D. 1565-1715, overlapping the Late Maunder Minimum (1675-1715), a period associated with cold conditions in southern Africa (Grodek et al., 2013). Similarly, the 5500-year palaeoflood record in the Orange River registered the most catastrophic floods between A.D. 1453 and 1785 (Zawada and Smith, 1991; Zawada, 2000), and farther south in the Buffels River flood frequency increased after A.D. 1600 in relation with cooler regional conditions (Benito et al., 2011b). In the Fish River, large floods were dated at 1640-1715, also coinciding with the Maunder Minimum (A.D. 1645-1715). Likewise, our Fish River palaeoflood record points to climate variability exerting some control on flood frequency, specifically a minor increase in flood frequency/magnitude during cold periods, which likely coincide with more seasonal rains. The distribution of these rains would cover extensive areas all over from the headwater in the escarpment to the Namib Desert, possibly indicating a general increase in water availability. Despite the strong interannual flow changes intrinsic to ephemeral rivers in arid and semiarid regions, our records show indications of lower (centennial) variability of the occurrence of extreme floods over the past three centuries.

6.2. Critical assessment of the 1972 flood discharge estimates

On 16 March 1972 a rapid filling of the Hardap Dam required the largest release of water ever from the flood gates to prevent uncontrolled overtopping. Because no gauging structures were located upstream of the dam, an inflowing flood hydrograph was estimated using gauge plate readings and controlled releases from the dam flood gates. The incoming flood, initially estimated at 6400 m^3s^{-1}, is the largest on record.

Determination of a robust discharge value, however, is critical for flood management in the catchment. Differing values of the 1972 peak discharge rate in the incoming flood hydrograph were reported, namely 6100 m^3s^{-1} by Kovacs (1988), 6400 m^3s^{-1} by NamWater (DWA), and 6800 m^3s^{-1} by Hattingh et al. (2011). Based on the original gauge plate reading, we carried out a new water balance, revisiting the flood gate releases, the emergency spill release, and an increase or reduction in dam capacity. The outcome of this analysis provided a maximum inflow discharge rate of 5500 m^3s^{-1}.

During the palaeoflood study performed at Vogelkranz, evidence was found of a flood peak of 4800 m^3s^{-1}, which passed down the Fish River in the 1970s. An additional source of flood water is the Packriem River (1700 km^2 in drainage area), a tributary of the Fish River with its confluence located directly upstream of the Hardap Dam. Therefore the 1972 flood, which entered the Hardap Dam, could have consisted of the 4800 m^3s^{-1} from the upper Fish River, which passed the Vogelkranz site, plus an additional contribution mainly from the Packriem River of ~700 m^3s^{-1} (13% of the total peak flow) for a peak flow of 5500 m^3s^{-1}. The additional contribution of the Pakriem River, with a specific discharge of 0.4 $m^3\ s^{-1}\ km^{-1}$, appears to be a reasonable figure.

6.3. Upper bound to floods magnitudes

The ubiquitous presence of old alluvial surfaces with stable flat topography provides valuable information about the largest stage of flooding in the study reach. The discharge estimation associated to flooded/non-flooded surface allows setting a UB magnitude of flooding, which can be incorporated in the flood frequency analysis. These high alluvial surfaces are typically composed of gravel and boulders for which exposed surfaces are coated by desert varnish. Desert or rock varnish is slow accreting (1–40 micron/ky) Mn, Fe and Si rich micron-size laminae on sub-aerially exposed rock surfaces (Perry and Adams, 1978), typically formed on regions with annual rainfall of 30-120 mm (Goldsmith et al., 2014). The detailed field inspection of homogenous desert varnish over exposed gravels and boulders in the Echo camp reach allows identifying high surfaces not affected by flood erosion over time intervals probably covering several millennia of little or no inundation. Here, in the Fish River Canyon, the UB flood indicators provide evidence that flooding over the past several thousand years has not exceeded 16,140 m^3s^{-1}, although this may be a conservative upper bound. In the upper Fish River catchment, upstream of the Hardap Dam, the identification of these non-flooded upper alluvial and bedrock surfaces was supported by the contrast with flooded gravel surfaces, as indicated by pocket accumulations of flood sand and silt. The non-inundated surfaces upstream of Hardap Dam indicate no floods for several hundred or thousand years with discharges greater than 6400 m^3s^{-1}, despite this value matching the largest flood discharged reported by by NamWater (DWA for Hardap Dam systematic record). The physical evidence of an upper bounded discharge of flooding was used to limit the extrapolation of the discharge associated to flood quantiles (Botero and Frances, 2010). The use of upper bounded distribution functions under the premise of maximum flood limit provided a robust characterization of the palaeoflood and systematic records.

Palaeoflood data can provide a significant extension of the instrumental data series to help define the maximum limit of flooding in the analysis of envelope curves (Enzel et al., 1993). In Namibia, the empirically established upper limit of the regional maximum floods (RMF) was described for Nambia by Kovaćs (1988) and more recently revised by Cloete et al. (2014). These regional enveloped curves were built from maximum monthly instantaneous flood peak data from 55 river gauging stations, and almost 1900 station years of gauged data (Cloete et al., 2014). Here, we plotted the maximum flood discharge vs drainage basin at northern, south and central-west, and Eastern Namibian regions (Fig. 11). The extended palaeoflood data records (HWMs and PSIs) plot on the upper range of flood discharges produced at any given catchment area. Fig. 11 shows that the number of flood data for catchments smaller than 100 km^2 is very limited. Hence, a potential application of palaeoflood records could complete the lack of knowledge on flood discharges from small ungauged catchments in Namibia.

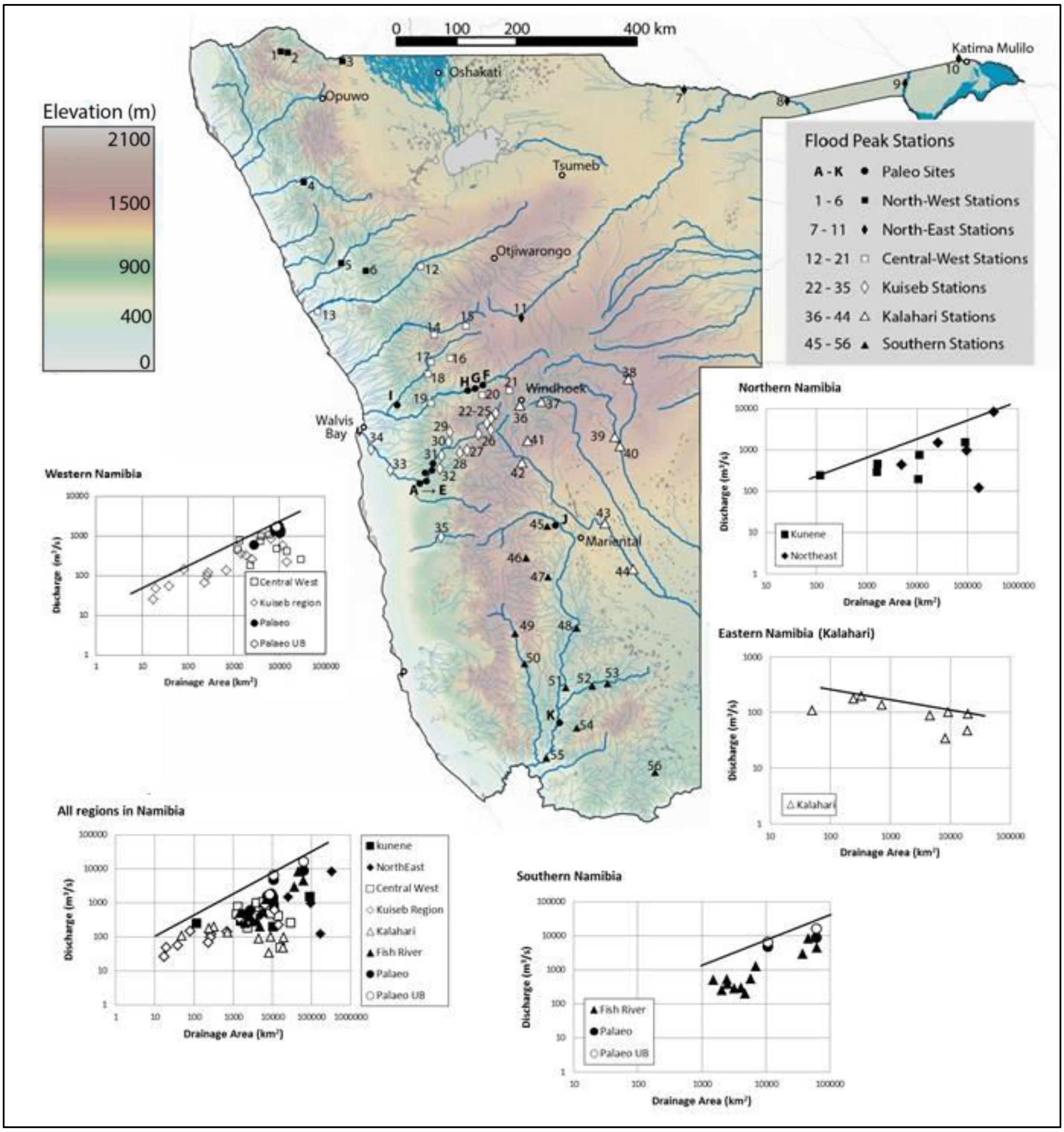

Fig. 11. Envelope curves in Nambia. Palaeo UB refers to upper bound floods (field evidence of non-exceedence elevation).

6.4. Extended flood records: implications for flood management and infrastructure design

Most of the large infrastructures, mainly dams, built or planned for Namibia are dimensioned on the basis of available systematic records and calculation of the Probable Maximum Flood. In the case of systematic records, the longest gauged data in the Fish River starts on 1961 (55 years) with little or scarce evidence on pre-instrumental observed or documented floods. According to the U.S. Bureau of Reclamation (1999), at-a-site stream flow data used for flood frequency relationhsip, limits the credible extrapolation for annual exceedance probability typically to 1%, and in optimal conditions to 0.5%. Extended flood records using systematic and palaeoflood information decrease the level of uncertainty of the quantile estimates, with optimal limit of credible extrapolation to 0.25% annual exceedence probability. Nevertheless, our observations and analyses corroborate the hypotheses that the largest flood in the Fish River systematic record (the 1972 flood) is probably the largest flood of the last few centuries.

The Hardap Dam was completed in 1962 with a reservoir capacity of 295 Mm^3 and supplies water to irrigate 3000 hectares of farmland near the town of Mariental. The dam is 34 m high and has a crest length of 865 m and crest a width of 6 m. Rehabilitation dam works have been performed in 1981 and 1994-1996 to prevent leakage through holes and cracking in the asphalt concrete sealing. The dam is equipped with four sluice-gated spillways with a combined discharge capacity of 4700 m^3s^{-1} at the high flood level of 1138.2 m (asl). At the non-overspill crest level of 1139.2 m (asl), a maximum discharge rate of 5000 m^3s^{-1} is achieved through the gated spillway, and an additional 1250 m^3s^{-1} over the auxillary spillway (Hattingh, 2007). Moreover, the early 1960s original dam design for the most extreme flood of 6400 m^3s^{-1} (exceedance probability of 0.1%) was close to estimates for the 1972 flood (5500-6400 m^3s^{-1}), casting doubt on the initial dam project calculations. The design floods for the Hardap Dam were re-evaluated by Hattingh (2007) as part of a dam safety assessment report commissioned by Ministry of Agriculture, Water and Forestry (MAWF). The revised flood peaks were calculated using the General Extreme Value (GEV) distribution function over the complete 65 year record (Table 4 ; Hattingh et al., 2011). The Hattingh' report concluded that the 18 years hydrological record used in the original dam project design resulted in under-sized spillway capacity, and discuss the need of more than 30 years record (from the actual 65 years record) to calculate the range of flood peak probabilities of exceedance. In their frequency analysis a discharge value of 6800 m^3s^{-1} was estimated for the 1972 flood peak, a figure that overestimates the peak flow entering the Hardap Dam according to our calculations of 5500 m^3s^{-1}, biasing flood frequency analysis results. Nonetheless, the extrapolation of a 65 year record to derive expected values of discharge of floods of 1000 to 5000 years return periods involves a high level of uncertainty.

In this regard, the value of paleoflood records is its potential to incorporate physical evidence of rare floods and limits on their largest magnitude over much longer time intervals. Palaeoflood hydrology has been used extensively by the U.S. Bureau of Reclamation (Ostenaa et al., 1996; Levish, 2002; England et al., 2010) in applying paleohydrological analysis toward dam-safety assessments. Flood frequency analysis with palaeoflood data shows higher discharge values than the ones obtained by Hattingh (2007) for relatively high probabilities of exceedance (>1%; Table 4). However, the palaeoflood statistical model gives lower discharges than Hattingh (2007) analysis for quantiles with low probabilities of exceedance (0.1%). In fact, the Hattingh's revised design of the 500-yr flood is on the order of the field evidence UB limit of discharge (i.e. ~7100 m^3s^{-1}) assuming an additional contribution of dicharge from the Packriem River. The safety evaluation flood peak (SEF) based on the probability of dam failure was calculated at 11,640 m^3s^{-1} (obtained empirically to represent probability of exceedance of 0.035%; Hattingh, 2007). Our upper bounds, tentatively estimated by lack of field evidence based on nonerosion evidence and nonvarnished rocks, indicate that this discharge was not exceeded for millennia. This SEF peak flow is 40% higher than the UB –observed by field evidence. From our results it is evident that the original design for the Hardap Dam does not fulfil safety criteria despite the reevaluation figures (Hattingh, 2007) overestimating flood quantiles according to our palaeoflood estimations. Current design flood (5000 m^3s^{-1}) and the safety check flood (6400

m^3s^{-1}) for the Hardap Dam are underestimated, and they should be modified to converge into 6000 m^3s^{-1} for design flood (0.1% exceedance probability) and 7000 m^3s^{-1} for the safety check flood (0.01% exceedance probability). Discharges obtained previously from SEF (11,640 m^3s^{-1}) overestimated the discharge results, and they do not provide a realistic estimation of dam safety features (dam and spillway designs).

7. Conclusions

The scarcity of flow gauge records in dryland ephemeral rivers is a major limitation in the assessment of flood hazards and water resources. This is of paramount importance given current interest in assessing the response of such rivers to future global change, especially when future climate scenarios predict reduced runoff but an increase in heavy rainfalls and flood hazards, as is the case for dryland regions of southern Africa (Milly et al., 2005; Kundzewicz et al., 2014). This paper presented a long-term flood record based on sedimentary flood deposists (palaeofloods) for the Fish River, the largest ephemeral river of Namibia. Two river reaches were studied: the upper catchment (Vogelkranz site) and the lower catchment within the Fish River Canyon (Echo Camp site). At each reach, stratigraphic sequences of flooding, ages (^{14}C, OSL) and flood discharges were established. In the Vogelkranz site there is sedimentary evidence of at least eight flood units deposited by flows with discharges >2300 m^3s^{-1} and four exceeding 3500 m^3s^{-1}. The oldest palaeoflood unit according to OSL dating was deposited 310 ±65 years ago (A.D. 1700 ±65). The largest flood discharge of 4800 m^3s^{-1} was marked by a tree log stuck in a crevice against the left margin cliff, likely corresponding to the 1972 flood according to the radiocarbon date. This flood was recorded at the Hardap Dam located downstream with a discharge previously estimated according to the dam level on 6400 m^3s^{-1}, and our calculations based on dam operation balance lowers the peak inflow to 5500 m^3s^{-1}. The peak flow difference between Vogelkranz and the Hardap Dam (13%) is attributed to the contribution from a tributary, the Pakriem River, entering the Fish River at the tail of the Hardap reservoir. In the Fish River Canyon (Echo Camp site) sedimentary evidence shows at least two large floods exceeding 8690 m^3s^{-1}, the oldest dated as 370 ±80 years ago (A.D. 1560-1720) deposited overlying a high alluvial surface. A set of at least 10-11 flood units were deposited at tributary mouths, post-dating an OSL age of 145 ±35 years ago (A.D. 1840-1900), the highest with minimum discharges of 3400 m^3s^{-1}. The palaeoflood chronology suggests that large floods occurred during the cold episode known as Minimum Maunder (A.D. 1650-1715) with subsequent flooding during the Little Ice Age (A.D. 1450-1850). The long-term picture of the palaeoflood record shows low variability on the occurrence of extreme floods over the last three centuries, which points out low regional flood sensitivity to past climate episodes in arid environments.

The flood frequency analysis using maximum likelihood estimators was carried out from annual maximum listed on instrumental records (SYS) and also combining gauged with palaeoflood data (PALEO+SYS). The two-component extreme value (TCEV) distribution function was successfully applied in both study reaches. The fitted distribution function shows an average return period of 300 and 100 years for the largest palaeoflood discharges (4800 and 8690 m^3s^{-1}) in the upper (Vogelkranz) and lower (Echo Camp) reaches respectively. The extrapolation of the distribution functions in the low exceedance probability quantiles (<0.1%) results in higher discharge values for the distribution fitted to only systematic data sets compared to the combined palaeoflood-and-systematic records. A second set of flood frequency analysis was carried out using UB distribution functions, namely LN4 distribution, with one parameter fixed to limit the highest maximum discharge. In a first approximation the discharges associated with the elevation of high alluvial surfaces with lack of flood evidence were used as palaeohydrological bounds (Levish, 2002). In the Vogelkranz the upper bounded surfaces provided a maximum discharge of 6400 m^3s^{-1}, whereas in the Echo Camp it was 16,140 m^3s^{-1}. The UB distribution functions provided the best performance to the combined PALEO+SYS data set, with a slower behaviour approaching the upper limit than the one fitted to the systematic record. The flood frequency analysis using centennial flood data sets were discussed in the context of dam safety evaluation calculated from traditional hydrological analysis, initially with 18-year gauge data sets and most recently reevaluated with a 65-year flood annual record. Our frequency analysis shows more conservative discharge values for the low probability quantiles (< 0.1%) than the conventional flood analysis. These results may have implications in relation to future plans to increase the capacity of the dam spillway to meet the current safety standards.

Acknowledgements

GB was supported through the MNCN (Spanish Research Council) without any specific grant. YE and TG thank the support of Hebrew University for the field work. The OSL dates are from the Laboratory of NP in the Geological Survey of Israel. We thank Lazarus Muhimba for surveying the cross sections in the river reaches and NamWater for providing transport during fieldwork in the Fish River. The reviewers are also thanked for their constructive comments which improved the manuscript.

References

Aitken, M.J., 1998. An Introduction to Optical Dating. New York: Oxford University Press.

Baker, V.R., 1987. Paleoflood hydrology and extreme flood events. Journal of Hydrology 96, 79–99.

Baker, V.R., 2008. Paleoflood hydrology: origin, progress, prospects. Geomorphology 101(1–2), 1–13.

Baker, V.R., Kochel, R.C., 1988. Flood sedimentation in bedrock fluvial systems. In: Baker, V.R., Kochel, R.C., Patton, P.C. (Eds.), Flood Geomorphology. John Wiley & Sons Ltd., U.S.A., pp. 123–137.

Baker, V.R., Webb, R.H., House, P.K., 2002. The Scientific and societal value of paleoflood hydrology. In: P.K., House, R.H., Webb, V.R., Baker, D.R. Levish (eds.), Ancient Floods, Modern Hazards: Principles and Applications of Paleoflood Hydrology. Water Science and Application Se-ries, vol. 5, 127–146. Washington, DC: American Geo-physical Union.

Benito G., O'Connor, J.E., 2013. Quantitative Paleoflood Hydrology. In: Shroder, J.F. (ed-in-chief), Wolh, E. (Volume Ed.) Treatise on Geomorphology, Volume 9, San Diego: Academic Press. 459–474.

Benito, G., Sánchez-Moya, Y., Sopeña, A., 2003. Sedimentology of high-stage flood deposits of the Tagus River, Central Spain. Sedimentary Geology 157, 107–132.

Benito, G., Rohde R.F., Seely, M., Kulls C., Dahan, O., Enzel, Y., Todd, S., Botero, B., Grodek, T., 2010. Management of alluvial aquifers in two southern African ephemeral rivers: Implications for IWRM. Water Resources Management Water Resources Management 24, 641–667.

Benito, G., Botero, B.A., Thorndycraft, V.R., Rico, M.T., Sánchez-Moya, Y., Sopeña, A., Machado, M.J., Dahan, O., 2011a. Rainfall-runoff modelling and palaeoflood hydrology applied to reconstruct centennial scale records of flooding and aquifer recharge in ungauged ephemeral rivers. Hydrology and Earth System Sciences 15, 1185–1196.

Benito, G., Thorndycraft, V.R., Rico, M.T., Sánchez-Moya, Y., Sopeña, A., Botero, B.A., Machado, M.J., Davis, M., Pérez-González, A., 2011b. Hydrological response of a dryland ephemeral river to southern African climatic variability during the last millennium. Quaternary Research 75, 471–482.

Botero, B. A., Francés, F., 2010. Estimation of high return period flood quantiles using additional non-systematic information with upper bounded statistical models, Hydrol. Earth Syst. Sci., 14, 2617–2628, doi:10.5194/hess–14–2617–2010, 2010.

Chase, B.M., Meadows, M.E., Scott, L., et al. 2009. A record of rapid Holocene climate change preserved in hyrax middens from southwestern Africa. Geology 37, 703–706.

Cloete, G.C., Basson, G.R., Sinske, S.A., (2014). Revision of Regional Maximum Flood (RMF) Estimation in Namibia. Journal SA Water. 40 (3) 535–548.

Crerar, S., Maré, H.G., 2005. Pre-Feasibility Study into Measures to Improve the Management of the Lower Orange River. LORC ref. no. : 97331/3485.

Dahan, O., Tatarsky, B., Enzel, Y., Kulls, C., Seely, M., Benito, G., 2008. Dynamics of flood water infiltration and ground water recharge in hyperarid desert. Ground Water. 46 (3), 450–461.

England, J.F., Jr., Klawon, J.E., Klinger, R.E., Bauer, T.R., 2006. Flood Hazard Study, Pueblo Dam, Colorado. Final Report, Bureau of Reclamation, Denver, CO, June, 160 pp.

England, J.F., Jr., Godaire, J.E., Klinger, R.E., Bauer, T.R., 2010. Paleohydrologic bounds and extreme flood frequency of the Arkansas River Basin, Colorado, USA. Geomorphology 124, 1–16. http://dx.doi.org/10.1016/j.geomorph.2010.07.021.

Enzel, Y., Ely, L.L., House, P.K., Baker, V.R., 1993. Paleoflood evidence for a natural upper bound to flood magnitudes in the Colorado river basin. *Water Resources Research* 29: 2287–2297.

Enzel, Y., Ely, L.L., Martinez-Goytre, J., Vivian, R.G., 1994. Paleofloods and a dam-failure flood on the Virgin River, Utah and Arizona. *Journal of Hydrology*, 153(3). 291–315.

Geological Survey. 1980. South West Africa / Namibia: Geological Map 1: 1 000 000.

Goldsmith, Y., Stein, M., Enzel, Y., 2014. From dust to varnish: Geochemical constraints on rock varnish formation in the Negev Desert, Israel, Geochimica et Cosmochimica Acta, 126, 97-111, 10.1016/j.gca.2013.10.040.

Greenbaum, N., Schwartz U., Benito, G., Porat, N., Cloete, G.C., Enzel, Y., (2014). Paleohydrology of extraordinary floods along the Swakop River, Namib Desert and paleoclimate implications. Quaternary Science Reviews 103, 153–169.

Grodek, T., Benito G., Botero, B.A., Jacoby, Y., Porat, N., Haviv, I., Cloete, G., Enzel, Y., 2013. The last millennium largest floods in the hyperarid Kuiseb River basin, Namib Desert. Journal of Quaternary Science, 28(3) 258–270.

Harden, T.M., O'Connor, J.E., Driscoll, D.G., Stamm, J.F., 2011. Flood-frequency analyses from paleoflood investigations for Spring, Rapid, Boxelder, and Elk Creeks, Black Hills, western South Dakota: U.S. Geological Survey Scientific Investigations Report 2011–5131, 136 pp.

Hattingh, L.C. 2007. Flood risk reduction: Mariental Town and Hardap Irrigation scheme. Dam Safety Final Report 11/11/3/1/2/H05. WRP Consulting Engineers, Pretoria, South Africa.

Hattingh, L., Cloete, G., Mostert, A., Muir, C., 2011. The impact of hydrology on the adequacy of existing dam standards- the Namibian experience. In: Romero Garcia et al. (eds.). Dam Maintenance and Rehabilitation II. Taylor & Francis Group, London. pp. 383–389. DOI: 10.1201/b10570–12.

Heine, K., 2004. Flood reconstructions in the Namib Desert, Namibia and Little Ice Age climatic implications: Evidence from slackwater deposits and desert soil sequences. Journal of the Geological Society of India, 64, 535–547.

Heine, K., 1987. Jungquartäre fluviale Geomorphodynamik in der Namib, Südwestafrika/Namibia. Zeitschrift für Geomorphologie, Suppl. v.66, pp.113–-134.

Heine, K., Völkel, J., 2010. Soil Clay Minerals in Namibia and their Significance for the Terrestrial and Marine Past Global Change Research. African Study Monographs, Suppl. 40. 31–50.

Heine, K., Völkel, J., 2011. Extreme floods around A.D. 1700 in the northern Namib Desert, Namibia, and in the orange river catchment, South Africa – were they forced by a decrease of solar irradiation during the little ice age? Geographia Polonica, 84, 61–80.

Henschel, J.R., Burke, A., Seely, M., 2005. Temporal and spatial variability of grass productivity in the central Namib Desert. African Study Monographs Suppl. 30, 43–56.

Heyns, P., 2005. Water institutional reforms in Namibia. Water Policy, 7, 2005, 89–106.

Hydrologic Engineering Center, 2010. HEC-RAS 4.1, River Analysis System, Hydraulics Version 4.1. Reference Manual, (CPD-69), U.S. Army Corps of Engineers, Davis, 411 pp. http://www.hec.usace.army.mil/software/hec-ras/hecras-document.html.

Jacobsen, P.J., Jacobsen, K.M., Seely, M.K., 1995. Ephemeral rivers and their catchments. Desert Research Foundation of Namibia, Windhoek.

Jarrett, R. D., England, J. F., Jr., 2002, Reliability of paleostage indicators for paleoflood studies. In: House, P.K., Webb, R.H., Baker, V.R., Levish, D.R. (Eds.), Ancient Floods, Modern Hazards: Principles and Applications of Paleoflood Hydrology. Water Science and Application Series, Vol. 5, American Geophysical Union, Washington, DC, pp. 91–109.

Kijko, A., 2004. Estimation of the Maximum Earthquake Magnitude-Mmax, Pure Appl. Geophys., 161, 1–27.

Kochel, R.C., Baker, V.R., 1988. Paleoflood analysis using slack water deposits. In: Baker, R.V., Kochel, R.C., Patton, P.C. (Eds.), Flood Geomorphology. Wiley, New York, NY, pp. 357–376.

Kovaćs, Z., 1988. Regional Maximum Floodpeaks in Southern Africa. Technical Report TR 137, Directory of Hydrology, Department of Water Affairs, Pretoria, South Africa.

Kundzewicz, Z. W., Kanae, S., Seneviratne, S.I., Handmer, J., Nicholls, N., Peduzzi, P., Mechler, R., Bouwer, L.M., Arnell, N., Mach, K., Muir-Wood, R., Brakenridge, G.R., Kron, W., Honda, Y., Benito, G., Takahashi, K., Sherstyukov, B., 2014. Flood risk and climate change – global and regional perspectives. Hydrological Sciences Journal 59 (1), 1–28.

Levish, D.R., 2002. Paleohydrologic bounds: nonexceedance information for flood hazard assessment. In: House, P.K., Webb, R.H., Baker, V.R., Levish, D.R. (Eds.), Ancient Floods, Modern Hazards: Principles and Applications of Paleoflood Hydrology. Water Science and Application Series. American Geophysical Union, Washington, DC, Vol. 5, pp. 175–190.

MAWF (Ministry of Agriculture, Water and Forestry), 2008. Strategic Plan 1008/8 to 2012/13, Windhoek, Namibia, 67 pp. http://www.iwrm-namibia.info.na/

Mendelsohn, J., Jarvis, A., Roberts, C., Robertson, T. 2002. Atlas of Namibia. David Phillips Publishers, Cape Town.

Milly, P.C.D., Dunne, K.A., Vecchia, A.V., 2005. Global pattern of trends in streamflow and water availability in a changing climate, Nature, 438, 347–350, doi:10.1038/nature04312.

Morin, E., Grodek, T., Dahan, O., Benito, G., Kulls, C., Jacoby, Y.,Van Langenhove, G., Seely, M., Enzel, Y., (2009). Flood routing and alluvial aquifer recharge along the ephemeral arid Kuiseb River, Namibia. Journal of Hydrology, 368, 262–275.

Murray, A.S., Wintle, A.G., 2000. Luminescence dating of quartz using an improved signle-aliquot regenerative-dose protocol. Radiation Measurements 32: 57–73.

Nicholson, S.E. 2001. A Semi-Quantitative, Regional Precipitation Data Set for Studying African Climates of the Nineteenth Century, Part I. Overview of the Data Set. Climatic Change, Volume 50, Number 3, pp. 317–353, August 2001. DOI: 10.1023/A:1010674724320.

O'Connell, D.R.H., Ostenaa, D.A., Levish, D.R., Klinger, R.E., 2002. Bayesian flood frequency analysis with paleohydrologic bound data. Water Resources Research 38, 1058. http://dx.doi.org/10.1029/2000WR000028.

Ostenaa, D., Levish, D., 1996. Reconnaissance paleoflood study for Ochoco Dam, Crooked River Project, Oregon: Seismotectonic. Report 96–2, Denver: U.S. Bureau of Reclamation, Seismotectonic and Geophysics Group.

Perry, R.S., Adams, J., 1978. Desert varnish: evidence for cyclic deposition of manganese. Nature 276, 489–491.

Porat, N., 2006. Use of magnetic separation for purifying quartz for luminescence dating. Ancient TL 24: 33–36.

Potter, W.D., 1958. Upper and lower frequency curves for peak rates of runoff. EOS Trans. AGU 39, 100-105.

Rossi, F., Fiorentino, M., Versace, P., 1984. Two-component Extreme Value Distribution for Flood Frequency Analysis, Water Reour. Res., 20 (6), 847–856.

Stedinger, J.R., Baker, V.R., 1987. Surface water hydrology: historical and paleoflood information. Reviews of Geophysics, 25, 119–124.

Stedinger, J. R., Cohn, T. A., 1986. Flood Frequency Analysis with Historical and Paleoflood Information, Water Resour. Res., 22(8), 785–793.

Stengel, H.W., 1964. The rivers of the Namib and their discharge into the Atlantic, Part 1: Kuiseb and Swakop. Scientific Papers of the Namib Desert Research Station 22.

Stengel, H.W., 1972. Historical floods: Notes on historical flood events and related fields. Flood capacities observed in rivers at various sites. Department of Water Affairs. Loose leaf 31cm. 89/1416

Strohbach, B.J., 2001. Vegetation Survey of Namibia. Journal of the Namibia Scientific Society 49: 93-124.

Swart, R., 2008. An earth science review of the Orange-Fish River Basin, Namibia. Unpublished report, Ephemeral River Basins in Southern Africa (ERB) Project, Desert Research Foundation of Namibia, Windhoek.

Takara, K., Loebis, J., 1996. Frequency Analysis Introducing Probable Maximum Hydrologic Events: Preliminary Studies in Japan and in Indonesia, in: Proceedings of International Symposium on Comparative Research on Hydrology and Water Resources in Southeast Asia and the Pacific, Yogyakarta, Indonesia, 18–22 November 1996, Indonesian National Committee for International Hydrology Programme, 67–76.

Tyson, P.D., Lindesay, J.A., 1992. The climate of the last 2000 years in southern Africa. The Holocene 2, 271–278.

Tyson P.D., Karlén, W., Holmgren, K., Heiss, G.A., 2000. The Little Ice Age and medieval warming in South Africa. South African Journal of Science 96, 121–126

U.S. Bureau of Reclamation, 1999. A framework for characterizing extreme floods for dam safety risk assessment. Prepared by Utah State University and Bureau of Reclamation, Denver, Colorado, p. 67.

Webb, R.H., Jarrett, R.D., 2002. One-dimensional estimation techniques for discharges of paleofloods and historical floods. In: House, P.K., Webb, R.H., Baker, V.R., Levish, D.R. (Eds.), Ancient Floods, Modern Hazards: Principles and Applications of Paleoflood Hydrology. Water Science and Application Series, Vol. 5, American Geophysical Union, Washington, DC, pp. 111-125.

Wessels, P., 2014. Personal communication, November 2014. Specialist Engineer, Directorate Hydrological Services, Department of Water Affairs and Sanitation, Pretoria, South Africa.

Williams, G.P., Costa, J.E., 1988. Geomorphic measurements after a flood. In: Baker, R.V., Kochel, R.C., Patton, P.C. (Eds.), Flood Geomorphology. Wiley, New York, NY, pp. 65–77.

Zawada, P.K., 2000. Palaeoflood Hydrological Analysis of Selected South African Rivers. Memoir of the Council for Geoscience, South Africa,

Zawada, P.K., Smith, A.M., 1991. The 1988 Orange River flood, Upington region, northwestern Cape Province, RSA. Terra Nova, 3, 317-324.